8-2011

Historical diversification of montane herpetofauna within and between the sierras of Mexico

Robert William Bryson Jr.
University of Nevada, Las Vegas

HISTORICAL DIVERSIFICATION OF MONTANE HERPETOFAUNA WITHIN AND BETWEEN THE SIERRAS OF MEXICO

By

Robert William Bryson, Jr.

A dissertation submitted in partial fulfillment
of the requirements for the

Doctor of Philosophy in Biological Sciences

School of Life Sciences
College of Sciences
The Graduate College

University of Nevada, Las Vegas
August 2011

THE GRADUATE COLLEGE

We recommend the dissertation prepared under our supervision by

Robert William Bryson, Jr.

entitled

Historical Diversification of Montane Herpetofauna Within and Between the Sierras of Mexico

be accepted in partial fulfillment of the requirements for the degree of

Doctorate of Philosophy in Biological Sciences
School of Life Sciences

Brett R. Riddle, Committee Chair

John Klicka, Committee Member

Brian Hedlund, Committee Member

Stephen M. Roland, Graduate College Representative

Ronald Smith, Ph. D., Vice President for Research and Graduate Studies
and Dean of the Graduate College

August 2011

ABSTRACT

Historical Diversification of Montane Herpetofauna Within and Between the Sierras of Mexico

by

Robert W. Bryson, Jr.

Dr. Brett R. Riddle, Examination Committee Chair
Professor of Biological Sciences
University of Nevada, Las Vegas

The Mexican highlands consist of four major mountain ranges spanning most of mainland Mexico. The evolutionary history of the Mexican highlands has been shaped by various geological and climatic events over the past several million years. The relative impacts of these historical events on diversification in montane taxa, however, remains uncertain. I used mitochondrial DNA data from three widely distributed species complexes of lizards as a model system to exemplify the potential roles of Neogene mountain formation and Quaternary climate change on timing and tempo of diversification across the Mexican highlands. My results suggested strong geographic partitioning of genetic variation across Mexico in all three lizard groups. There appeared to be a generalizable anchor of diversification across taxa centered around the development of the Transvolcanic Belt. Diversification across the rest of the Mexican highlands was largely idiosyncratic, but filter barriers such as river drainages likely subdivided lineages differentially through time. Diversification patterns observed in my three focal groups of lizards provide additional insight into the mechanisms that impacted differentiation of highland taxa across the complex Mexican highlands.

ACKNOWLEDGMENTS

I am greatly indebted to my dissertation committee for their support, advice, and encouragement throughout my tenure as a graduate student at UNLV: Drs. Brett Riddle, John Klicka, Brian Hedlund, Jonathan Campbell, and Steve Rowland. Brett gave me a second chance in the School of Life Sciences, and I am grateful for the opportunity he presented to me. Research in Mexico would not have been possible without the support of numerous friends and colleagues in Mexico, including Dr. David Lazcano, Dr. Adrian Nieto, Uri Garcia, Dr. Javier Alvarado, Dr. Gustavo Quintero, Paulino Ponce, Jason Jones, Chris Grunwald, and especially the late Fernando Mendoza. Without Fernando's support and enthusiasm, none of this would have been possible. Many, many people contributed their time and help in the field, and I hope that I have acknowledged them properly in my publications. I would like to thank the UNLV Systematics Group, Brian Smith, Tereza Jezkova, Dr. Jef Jaeger, Derek Houston, Stacy Mantooth, Sean Neiswenter, Matt Graham, Viki Hemmings, Dr. Lois Alexander, and Mallory Eckstut for their contributions to my intellectual growth. Last, and of course not least, I thank my amazing family. They nervously awaited for my safe return back to the US after my many expeditions to Mexico, and always supported me. To my wife, Meg, words can never express my gratitude for the overwhelming support and love you have given to me throughout the years.

My research was largely supported through funds made available by UNLV (Barrick Fellowship, Graduate and Professional Student Association grants, Graduate ACCESS grants, and International Studies scholarships). I received additional important funding from T&E Inc. (Conservation Biology Research Grant), the American Museum

of Natural History (Theodore Roosevelt Fund), and the Southwestern Association of Naturalists (Howard McCarley Student Research Award). Several institutions provided important tissue samples, including the American Museum of Natural History, Louisiana State University, Museum of Vertebrate Zoology, Texas Museum of Natural History, Universidad Nacional Autónoma de México, Universidad Autónoma de Nuevo León, and University of Texas at Arlington.

TABLE OF CONTENTS

LIST OF TABLES

LIST OF FIGURES

CHAPTER 1

INTRODUCTION

The Mexican highlands span a broad transition zone between temperate and tropical biotas, and combined with their complex topography and dynamic tectonic and climatic history, provide a matrix for the evolution of a spectacularly diverse biota. The Mexican highlands consist of four major mountain ranges traversing most of mainland Mexico (Fig. 1.1), including the north-to-south trending Sierra Madre Occidental and Sierra Madre Oriental of northern Mexico, and the east-west trending Transvolcanic Belt and Sierra Madre del Sur in central and southern Mexico. The evolutionary history of the Mexican highlands has been shaped by various geological and climatic events over the past several million years. The relative impacts of these historical events on diversification in montane taxa, however, remains uncertain owing in part to the paucity of studies on broadly distributed highland taxa.

Ancient development over 30 million years ago of most of the major mountains in Mexico probably pre-dates diversification of the extant highland-adapted species. Neogene formation of the Transvolcanic Belt during the Miocene and Pliocene, however, undoubtedly affected both the timing and tempo of diversification in many montane species. This volcanic chain of mountains is one of the predominant geographical features of Mexico, and its geological development has been posited as a primary contributor to the biogeographic histories of numerous taxa. Causal mechanisms driving diversification across the remaining Mexican sierras is less clear, but may be associated with a number of barriers differentially subdividing lineages through time, as well as highland habitat change associated with Pleistocene glacial–interglacial cycles.

For my dissertation research, I examined the genetic structuring of three co-distributed species groups of lizards with wide distributions across the highlands of Mexico. I reconstructed maternal history and estimated dates of lineage divergences using mitochondrial DNA data. In my second chapter, I explored lineage diversification in the mountain horned lizard (*Phrynosoma orbiculare*), and compared results to patterns of diversification observed in co-distributed taxa. In my third chapter, I tested the hypothesis of diversification rate shifts in bunchgrass lizards (*Sceloporus scalaris* group) in response to periods of development of the Transvolcanic Belt and Pleistocene glacial–interglacial cycles. In my final chapter, I investigated the tempo and mode of diversification in alligator lizards in the genus *Barisia*. Insight gained from my dissertation research provides additional insight into the mechanisms that impacted differentiation of highland taxa across the complex Mexican highlands.

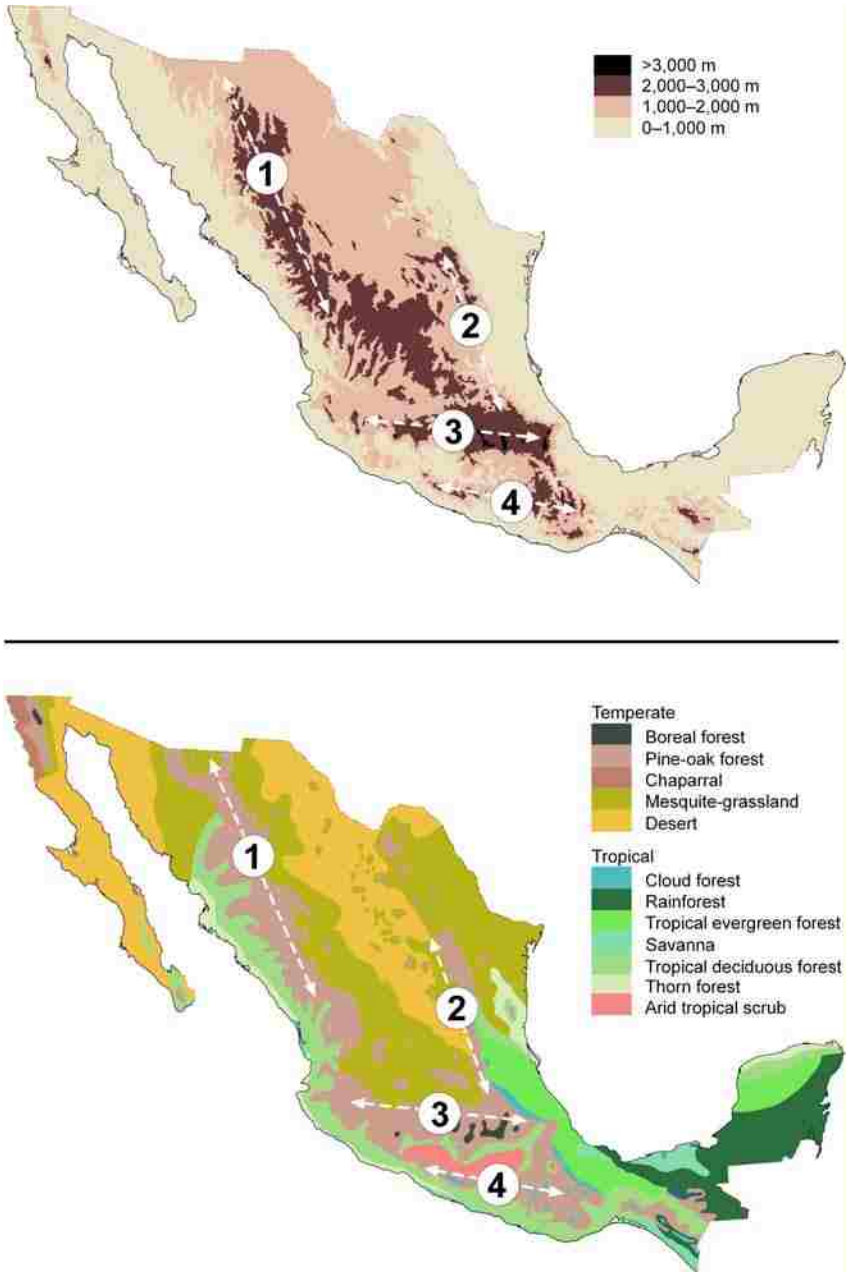

Figure 1.1. Major mountains of Mexico. 1) Sierra Madre Occidental, 2) Sierra Madre Oriental, 3) Transvolcanic Belt, and 4) Sierra Madre del Sur. Adapted from Campbell and Lamar (2004).

CHAPTER 2

DIVERSIFICATION IN THE MEXICAN HORNED LIZARD *PHRYNOSOMA ORBICULARE*

Introduction

The Mexican highlands harbor a significant amount of the world's biodiversity (Ramamoorthy et al., 1993; Mittermeier et al., 2005) and a high level of biotic endemicity (Peterson et al., 1993). Despite considerable attention and decades of biogeographic study, a general model describing the historical processes that generated this diversity continues to remain elusive. Geological history, dynamic climate change, and complex topography have synergistically driven what appears to be an array of either taxon-specific or general shared responses (Sullivan et al., 2000; Bryson et al., 2011a). Neogene vicariance in the Miocene and Pliocene and Quaternary climate change have each shaped the geographic distribution of genetic variation in co-distributed highland taxa, yet the relative impacts of these historical processes on lineage diversification appear to differ between lineages (Bryson et al., 2011a; Bryson et al., 2011b; Bryson et al., in press).

Deciphering the events that have shaped present-day biological diversity in the Mexican highland system requires an accounting for considerable historical complexity. Formation over 30 million years ago (Ma) of three of the four major mountain ranges in Mexico (Sierra Madre Occidental, Sierra Madre Oriental, and Sierra Madre del Sur; Ferrusquía-Villafranca and González-Guzman, 2005) probably predates diversification in extant highland-adapted lineages. Estimated Neogene divergences in highland taxa within these ranges (Zaldivar-Riverón et al., 2005; Weir et al., 2008; Bryson et al., 2011b) suggest then that events other than mountain uplifting drove pre-Quaternary

diversification. A number of studies have identified filter barriers such as river drainages within the major sierras (reviewed in Bryson et al., 2011a). It remains unclear, however, how effective these barriers were in dividing lineages through history, and when these barriers were relevant in splitting lineages. Diversification associated with the Neogene uplift of the Transvolcanic Belt appears more tractable. Unfortunately, the complex history of this volcanic mountain range (Gómez-Tuena et al., 2007) makes accurate dating of vicariant events presumably responsible for divergences among co-distributed taxa difficult.

Quaternary climate change has been posited as a major driver of biological diversification in North America (Hewitt, 2004). In Mexico, montane vegetation may have expanded downward at least 1000 m during Pleistocene glacial periods (McDonald, 1993), and linked previously isolated highland biotas (McDonald, 1993; Marshall and Liebherr, 2000). Subsequently, during interglacial episodes, highland woodlands retracted and their associated biota became isolated (Anducho-Reyes et al., 2008). Repeated throughout the Pleistocene, these habitat shifts triggered range-wide divergences in many highland taxa across Mexico (León-Paniagua et al., 2007; Anducho-Reyes et al., 2008; Kerhoulas and Arbogast, 2010; Bryson et al., in press).

The widespread horned lizard *Phrynosoma orbiculare* represents an ideal species to investigate the relative impacts of Neogene vicariance and Quaternary climate change on lineage diversification across the Mexican highlands. It is endemic to Mexico, and broadly associated with mixed pine-oak woodlands in the Sierra Madre Occidental, Sierra Madre Oriental, and Transvolcanic Belt, and semiarid shrubland on the Central Mexican Plateau (Sherbrooke, 2003) (Fig. 1). Further, it is thought to be one of the oldest extant

species of *Phrynosoma*, dating back to the Miocene (Presch, 1969; Montanucci, 1987). Thus, *P. orbiculare* has had a long history in Mexico.

Here I used mixed-model phylogenetic analyses of mitochondrial DNA (mtDNA) to examine the maternal history of *P. orbiculare*. Mitochondrial DNA, despite potential limitations (e.g. Edwards and Bensch, 2009), appears useful for detecting recent geographic patterns (Moore, 1995; Hudson and Coyne, 2002; Zink and Barrowclough, 2008; Barrowclough and Zink, 2009). This marker can also lead to significant biogeographic discoveries (e.g. Upton and Murphy, 1997; Riddle et al., 2000a), and is an important tool for exploring the genetic consequences of ecological history (e.g. Wiens et al., 2007; Burney and Brumfield, 2009; Pyron and Burbrink, 2009). I formulated a robust hypothesis of matrilineal relationships based on range-wide sampling of *P. orbiculare*, and estimated dates of lineage divergences from a relaxed molecular clock to provide a probabilistic temporal calibration for the phylogeny. I compared the phylogeographic signal evident in *P. orbiculare* to other co-distributed highland taxa to aid in the interpretation of historical biogeographic events that may have broadly impacted taxa across the Mexican highlands.

Methods

Taxon sampling and DNA sequencing

I obtained tissues from 36 *P. orbiculare* (Table 1) from across its distribution (Fig. 1). The number and distribution of subspecies of *P. orbiculare* has varied historically (Horowitz, 1955; McDiarmid, 1963; Montanucci, 1979). Because of the

uncertainty regarding delimitation of subspecies (McDiarmid, 1963) and to frame my results in terms of geography rather than taxonomy, I simply referred to specimens as *P. orbiculare*, consistent with usage in field guides (e.g., Lemos-Espinal and Smith, 2007a, 2007b; Dixon and Lemos-Espinal, 2011). I used *P. modestum* and *P. douglasii* as outgroups (Leaché and McGuire, 2006; Weins et al., 2010).

I sequenced two mtDNA gene regions, including NADH dehydrogenase subunit 4 and flanking tRNAs (ND4) and ATPase subunits 8 and 6 (ATPase 8, ATPase 6). These gene regions have previously been shown to be informative at different levels of divergence within lizards (Leaché and Mulcahy, 2007; Lindell et al. 2008). Total genomic DNA was extracted from liver or tail clips using the QIAGEN DNeasy Blood and Tissue Kit (Qiagen, Valencia, CA) following manufacturer's recommendations. All gene regions were amplified via PCR in a mix containing 6.25 µl Takara ExTaq Polymerase Premix (Takara Mirus Bio Inc., Madison, WI, USA), 4.25 µl double-distilled water, 0.5 µl each primer (10 µl), and 1.0 µl of template DNA. Primer sequences for ND4 are given in Arévalo et al. (1994), and for ATPase were specifically designed for this project (C2LF, 5'– ATCTGCGGGTCAAACCACAG–3'; C3LR, 5'– GCGTGTGYTTGGTGGGTCAT–3'). DNA was denatured initially at 95 °C for 2.5 min; 35–40 cycles of amplification were then performed under the following conditions: denaturation at 95 °C for 1 min, annealing at 56 °C for 1 min, and extension at 72 °C for 1 min; this was followed by a final 10 min elongation at 72 °C. Double-stranded PCR amplified products were checked by electrophoresis on a 1% agarose gel, purified using exonuclease and shrimp phosphatase, and directly sequenced in both directions with the amplification primers using a Big Dye Terminator v. 3.1 cycle sequencing kit (Applied

Biosystems, Foster City, CA, USA). The completed sequencing reactions were cleaned of excess dyes using CentriSep spin columns (Princeton Separations, Inc., Adelphia, NJ), and sequences were visualized on an ABI Prism 3130 capillary autosequencer. Forward and reverse sequences for each individual were edited and manually aligned using Sequencher 4.2 (Gene Codes Corporation, Ann Arbor, MI).

Phylogenetic inference

I analyzed my sequence data using Bayesian inference (BI) and maximum likelihood (ML) phylogenetic methods. Bayesian inference analyses were conducted using MrBayes 3.1 (Ronquist and Huelsenbeck, 2003) on the combined mtDNA dataset, implementing separate models for each gene region (ND4, tRNAs, ATPase 8, ATPase 6). MrModeltest 2.1 (Nylander, 2004) was used to select a best-fit model of evolution, based on Akaike Information Criteria (AIC), for each partition. Bayesian settings included random starting trees, a variable rate prior, a mean branch length exponential prior of 50, and heating temperature of 0.06. Analyses consisted of four runs (nruns=4) conducted each with three heated and one cold Markov chain sampling every 100 generations for 4 million generations. Output parameters were visualized using the program TRACER v1.4 (Rambaut and Drummond, 2007) to ascertain stationarity and whether the duplicated runs had converged on the same mean likelihood. Convergence was further assessed using AWTY (Nylander et al., 2008). All samples obtained during the first one million (25%) generations were discarded as burn-in. A 50% majority-rule consensus phylogram with nodal posterior probability support was estimated from the combination of the four runs post-burn-in. Maximum likelihood analyses were conducted using RAxML 7.0.3 (Stamatakis, 2006) with the same partitioning scheme used for the BI analyses. The

GTRGAMMA model was used, and 1000 nonparametric bootstrap replicates were performed to assess nodal support. I considered those nodes with ≥ 95% Bayesian posterior probability and ≥ 70% bootstrap support as strongly supported (Hillis and Bull, 1993; Felsenstein, 2004).

Divergence time estimation

Divergence dates were estimated using a relaxed Bayesian molecular clock framework implemented in BEAST v1.6.1 (Drummond and Rambaut, 2007). To reduce potential problems associated with model parameter variance across heterogeneous datasets (Ho, 2005; Guiher and Burbrink, 2008), divergence estimates were inferred for a reduced dataset, which included one individual from each geographically structured lineage of *P. orbiculare* inferred from BI analyses. Two different clock-calibration methods were used to obtain estimates. The first method utilized a relaxed uncorrelated lognormal clock and node constraints obtained from the fossil and geological record. To calibrate the tree, I included sequences from several outgroups (Table 1). The second method employed a substitution rate calibration and relaxed uncorrelated lognormal clock. I used a rate calibration for mtDNA previously calculated for a similar sized lizard (Macey et al., 1999). This substitution rate, here corrected to 8.05×10^{-3} substitutions/site/million year using a more complex GTR + G model, has been used in a number of studies to date divergences in lizards (e.g., Morando et al., 2004; Tennesson and Zamudio, 2008; Luxbacher and Knouft, 2009). Both datasets were partitioned by gene, and best-fit models of evolution were estimated using MrModeltest and unlinked across partitions.

For each clock-calibration method, analyses consisted of two independent runs each of 40 million generations, with samples retained every 1000 generations, and with a Yule tree prior. Results were displayed in TRACER to confirm acceptable mixing and likelihood stationarity, appropriate burn-in, and adequate effective sample sizes. After discarding the first 4 million generations (10%) as burn-in, the trees and parameter estimates from the two runs were combined using LogCombiner v1.6.1 (Drummond and Rambaut, 2007). The parameter values of the samples from the posterior distribution were summarized on the maximum clade credibility tree using TreeAnnotator v1.6.1 (Drummond and Rambaut, 2007), with the posterior probability limit set to zero and mean node heights summarized.

For calibrated analyses, I placed two calibration points with lognormal distributions on the tree as follows:

(a) At the stem of a short-horned lizard clade (*P. douglasii*, *P. hernandesi*, and *P. ditmarsi*), I placed the oldest known fossils referable to *P. douglasii* from the Early Miocene (Hemingfordian North American Land Mammal Age; Robinson and Van Devender, 1973; Van Devender and Eshelman, 1979; Estes, 1983). The stem was constrained with a zero offset (hard upper bound) of 16 Ma, a lognormal mean of 0.7, and a lognormal standard deviation of 0.5. This produced a median age of 18 Ma and a 95% prior credible interval (PCI) extending to the beginning of the Hemingfordian 20.6 Ma.

(b) At the stem of a desert horned lizard clade containing *P. platyrhinos, P. goodei*, and a related *Phrynosoma* from Yuma Proving Grounds, Arizona (*P*. "Yuma"; Mulcahy et al., 2006), I placed a calibration based on the Pliocene marine incursion of the Sea of Cortés and development of the Bouse Embayment. This geological event is

thought to have driven divergences in several co-distributed taxa (Lamb et al., 1989; Riddle et al., 2000b; Pellmyr and Segraves, 2003; Murphy et al. 2006; Castoe et al., 2007), including *P. platyrhinos* (Jones, 1995), and has been used as a calibration point for divergence dating in other studies (Castoe et al., 2009; Bryson et al., 2011a; Daza et al., 2010). The stem was given a lognormal mean of 1.1 and a lognormal standard deviation of 0.37, resulting in a median age centered at the climax of the formation of the Sea of Cortés and development of the Bouse embayment at 3 Ma, and a 95% PCI extending to the beginning of the development of the Sea of Cortés at 5.5 Ma (Carreño and Helenes, 2002, and references therein). No zero offset was used.

Results

Phylogenetic inference

The final dataset consisted of 1675 aligned nucleotide positions. Models of sequence evolution selected for the partitions were GTR + I + G (ND4), GTR + I (ATPase 8), GTR + G (ATPase 6), and HKY + I (tRNA). All sequences were deposited in GenBank.

From my phylogenetic analyses, I inferred 11 geographically structured, well supported mitochondrial lineages within *P. orbiculare* (Figs. 2–3). Samples from the Sierra Madre Occidental formed five geographically distinct lineages (I–V) contained in a larger 'northern clade'. Samples from the rest of the distribution formed my 'southern clade'. Distributions of lineages in the southern clade are as follows: southernmost extension of the Sierra Madre Oriental that overlaps parts of the eastern Transvolcanic

Belt (VI), central Transvolcanic Belt and adjacent sections of the Central Mexican Plateau (VII, VIII), southern Sierra Madre Oriental in eastern Hidalgo (IX), the western and southern portions of the Central Mexican Plateau (X), and northern Sierra Madre Oriental and adjacent foothills on the Central Mexican Plateau (XI).

Relationships among lineages were well supported, with the exception of one poorly supported node (73% posterior probability, 46% bootstrap) subtending the lineages from Chihuahua and the rest of the Sierra Madre Occidental (Fig. 2). However, in BEAST analyses on a reduced dataset (see below), this node received 100% posterior probability. Combined, I cautiously infer this to be a supported relationship. Within the southern clade, divergences followed a stepwise pattern (Fig. 3) from the southern end of the Sierra Madre Oriental (lineage VI), across the Transvolcanic Belt (sister lineages VII–VIII), up the Sierra Madre Oriental (lineage IX), across the Central Mexican Plateau (lineage X), and up to the northern Sierra Madre Oriental (lineage XI).

Divergence time estimation

The selected models of sequence evolution for the fossil-calibrated and rate-calibrated datasets were GTR + I + G (ND4, ATPase 8, ATPase 6, fossil-calibrated), GTR + I (ATPase 8, rate-calibrated), GTR + G (ATPase 6, rate-calibrated), HKY + I + G (tRNA, fossil-calibrated), and HKY + I (tRNA, rate-calibrated). Posterior probability support for inferred divergences within *P. orbiculare* were high; 100% between the northern and southern clades, 100% within the northern clade, and 94–100% within the southern clade. Dating estimates suggested that diversification in *P. orbiculare* probably began in the Late Miocene (Table 2, Fig. 4) with a basal divergence between the northern and southern clades. Several divergences appear to have followed in the Neogene,

including three sequential splits in the southern clade and two splits in the northern clade. My estimates place the remaining divergences, two in the southern clade and two in the northern clade, within a Pliocene–Pleistocene timeframe.

Discussion

Diversification patterns across the Transvolcanic Belt

Inferred spatial and temporal patterns of matrilineal diversification in *P. orbiculare* provide additional insight into the mechanisms that impacted differentiation of highland taxa across the Mexican highlands. Neogene vicariance had a relatively strong role in driving diversification within *P. orbiculare*. Six of the ten inferred lineage spitting events probably occurred during this time period (Fig. 4). The two oldest divergences within the southern clade, and perhaps initial diversification of *P. orbiculare*, are likely associated with major volcanic episodes along the Transvolcanic Belt. A recent revision summarizing the past two decades of research on the origin of the Transvolcanic Belt (Gómez-Tuena et al. 2007) suggested that the first major range-wide volcanic episode occurred about 10–19 Ma. Early diversification in *P. orbiculare* roughly 7.5 Ma might have followed this period of uplift. A subsequent period of marked widespread volcanism across the Transvolcanic Belt ensued around 7.5–3 Ma (Gómez-Tuena et al. 2007), and this second episode of volcanism likely caused the two oldest divergences within the southern clade of *P. orbiculare*, estimated to have occurred about 6 Ma and 5 Ma. These estimated dates are remarkably consistent with mean divergences around 5–7 Ma inferred for a suite of taxa distributed across the Transvolcanic Belt (toads, Mulcahy and

Mendelson, 2000; cichlids, Hulsey et al., 2004; Mexican jays, McCormack et al., 2008, 2011; montane rattlesnakes, Bryson et al., 2011a, Bryson et al., in press; gophersnakes, Bryson et al., 2011b). These shared temporal divergences suggest uplifting of the Transvolcanic Belt around 7.5–3 Ma broadly impacted a variety of taxa.

Diversification patterns within the northern sierras

Several mtDNA lineages of *P. orbiculare* are embedded within the Sierra Madre Occidental and Sierra Madre Oriental (Fig. 3). This finding is consistent with diversification patterns observed in several co-distributed taxa (Bryson et al., 2011a; Gugger et al., 2011; Bryson et al., in press). The fragmented topography and environmental heterogeneity within the Sierra Madre Occidental in concert with Quaternary climate change are likely driving diversification across this range (Salinas-Moreno et al., 2004). Deep river drainages may be acting as filter barriers to highland taxa. Previous studies (Salinas-Moreno et al., 2004; Anducho-Reyes et al., 2008; Bryson et al., 2011a) found the Rio Mezquital basin across southern Durango (Fig. 5) to be an isolating barrier. Two lineages of *P. orbiculare* also appear to be separated by this drainage. One lineage of *P. orbiculare* appears isolated in northern Nayarit. Interestingly, a geographically identical lineage was also found in montane rattlesnakes (Bryson et al., 2011a). In this region, the Rio Mezquital basin and headwater tributaries of the Rio Santiago basin (Fig. 5) may have carved an island of montane habitat isolated from the remainder of the southern Sierra Madre Occidental. In the Sierra Madre Occidental to the north, the combination of the Rio Culiacán basin across the Pacific slopes and the tributaries of the Rio Nazas basin across the interior slopes may be forming a disrupting barrier (Fig. 5) to some highland taxa. I observed a deep basal divergence within the

northern lineage of *P. orbiculare* across this region in northern Durango. A spatially congruent genetic break was also observed here in twin-spotted rattlesnakes (Bryson et al., in press). The inferred times of divergences, however, appear different (Table 3), suggesting this Rio Culiacán-Rio Nazas barrier may be differentially affecting lineage splitting through time. Similar incongruence was observed between other co-distributed taxa subdivided across breaks in the Sierra Madre Occidental (Table 3).

The Sierra Madre Oriental appears to be divisible into at least two unique sections (Luna-Vega et al., 1999; Salinas-Moreno et al., 2004). Several co-distributed highland taxa display distinct genetic breaks across central San Luis Potosí (Bryson et al., 2007; McCormack et al., 2008; Bryson et al., 2011a), including *P. orbiculare* (Fig. 3). There is a distinct absence of pines in this region (Farjon and Styles, 1997; Fig. 1), and the lowlands that cut across the Sierra Madre Oriental form the Cerritos-Arista and Saladan filter barriers (Morafka, 1977; Fig. 5). A probable Pleistocene divergence between lineages of *P. orbiculare* isolated north and south of this combined barrier is temporally consistent with most lineage splits observed in co-distributed taxa (Table 3). An older divergence in Middle American gophersnakes (Table 3) suggests this barrier may have been influential in driving divergences earlier in time as well. The Sierra Madre Oriental may also include a distinct southern segment in Puebla and Veracruz. This region has a complex geological history, and contains geological and biotic elements of both the Sierra Madre Oriental and Transvolcanic Belt (Marshall and Liebherr, 2000; Salinas-Moreno et al., 2004; Corona et al., 2007; Paniagua and Morrone, 2009). The Sierra Madre Oriental may have once been continuous from Hidalgo south into northern Oaxaca, and later divided by the formation of the Transvolcanic Belt (Corona et al.,

2007; Paniagua and Morrone, 2009). The inferred basal split in my southern clade of *P. orbiculare* around 5.5 Ma (Fig. 3) is consistent with this scenario.

Diversification patterns across the Central Mexican Plateau

Expansions of pine-oak woodlands across the Central Mexican Plateau during Pleistocene glacial periods (Gugger et al., 2011; Bryson et al., in press) may have promoted dispersal between highlands, resulting in contact between previously isolated taxa. Periodic bouts of gene flow during these periods could have erased or obscured previously acquired signals of historical isolation. Despite this potential, the distribution of the maternal lineage of *P. orbiculare* confined to the Central Mexican Plateau is largely congruent with regional genetic groups seen in other highland taxa (Fig. 6). These geographically overlapping lineages suggest similar responses to barriers across this region. However, the distributions of sister lineages to these Central Mexican Plateau lineages vary (Fig. 6), suggesting the Central Mexican Plateau is accumulating lineages from geographically different sources in different taxa. Potential shared barriers between Central Mexican Plateau lineages include the combined Cerritos-Arista/Saladan barriers to the northeast, the extensive Rio Pánuco basin to the east and the Rio Lerma basin to the south, and pine-oak habitat disjunctions to the west (Fig. 5). Given non-identical lineage ranges, however, soft allopatry through ecological vicariance may also explain these distributions (Pyron and Burbrink, 2010). Under this scenario, geological barriers limiting lineage distributions may not be evident. While an attractive alternative, a recent study on co-distributed Mexican jays (McCormack et al., 2010) found little evidence for ecological niche divergence between lineages of Mexican jays in the highlands of the northern Sierra Madre Oriental, Central Mexican Plateau, and Sierra Madre Occidental.

Additional phylogeographic studies on highland taxa with wide distributions across Mexico and subsequent analyses within a comparative framework are needed to better elucidate idiosyncratic versus general processes promoting lineage diversification across the Central Mexican Plateau and Mexican highlands.

Systematic and conservation implications

Although beyond the scope of this paper, my results based on mtDNA are largely in agreement with historical studies on morphology (Horowitz, 1955; Montanucci, 1979) and warrant some discussion. Congruence suggests several distinct lineages are embedded within *P. orbiculare*. Nearly precise overlapping distributions of my inferred lineages with morphologically distinct subspecies are as follows: (a) Lineages I-II from Chihuahua with *P. o. bradti* (sensu Horowitz, 1955); (b) Lineages III-V from the southern half of the Sierra Madre Occidental with *P. o. durangoensis* (Horowitz, 1955); (c) Lineages VII-VIII with *P. o. orbiculare*; and (d) Lineage XI with *P. o. oriental*. My remaining three mtDNA lineages represent *P. o. cortezii* (Lineages VI and IX) and *P. o. cortezii* and *P. o. dugesi* (Lineage X). Numerous intergrade zones between the various subspecies appear to exist (Horowitz, 1955; Montanucci, 1979) and to such a degree that *P. orbiculare* was considered one variable monotypic species (McDiarmid, 1963). Because mtDNA alone might not adequately measure gene flow in lizards (e.g. Godinho et al., 2008; Lindell et al., 2008), future studies should incorporate multilocus data to further delimit distributions of *P. orbiculare* lineages.

The International Union for Conservation of Nature (IUCN) considers *P. orbiculare* to be a species of least concern because of its wide distribution across Mexico and large population size (Mendoza-Quijano et al., 2007). The Mexican government

classifies this species as threatened (SEMARNAT, 2010). Treated as a single wide-ranging species, *P. orbiculare* is presumably buffered against anthropogenic disturbances. However, my findings suggest that *P. orbiculare* is in fact probably comprised of multiple distinct lineages. Some of these lineages, such as the one occurring in Veracruz and Puebla and the one in northern Nayarit (lineages III and VI, Fig. 3), appear to have small distributions and long independent evolutionary histories. Given the amount and rate of habitat destruction across the Mexican highlands (Challenger, 1998; Brower et al., 2002; Galicia and García-Romero, 2007), these range-restricted lineages merit additional consideration for protection.

Table 2.1. Collection and voucher data for genetic samples of *Phrynosoma* used in this study. All samples deposited in the Las Vegas Tissue Collection (LVT) or Texas Natural History Collection (TNHC). Asterisks denote outgroup samples used in fossil-calibrated divergence dating.

Taxon	Locality	Sample ID (MX)	Voucher Number
P. orbiculare	Mexico: Aguascalientes: Sierra Fría	1	LVT 10782
P. orbiculare	Mexico: Chihuahua: Colonia García	TZ	LVT 10794
P. orbiculare	Mexico: Chihuahua: El Pima, Mpo. Temosachic	27	LVT 10759
P. orbiculare	Mexico: Chihuahua: Mesa de Agostadero	161	LVT 10761
P. orbiculare	Mexico: Chihuahua: Ejido Zorillo	335	LVT 10760
P. orbiculare	Mexico: Chihuahua: Guachochi	398	LVT 10762
P. orbiculare	Mexico: Coahuila: Santa Rita	4	LVT 10791
P. orbiculare	Mexico: Coahuila: Ejido La Casita	165	LVT 10787
P. orbiculare	Mexico: Distrito Federal: San Pablo Oztotepec	400	LVT 10773
P. orbiculare	Mexico: Distrito Federal: Sierra Ajusco	447	LVT 10774
P. orbiculare	Mexico: Durango: Rancho Santa Barbara	5	LVT 10767
P. orbiculare	Mexico: Durango: E Topia	397	LVT 10766
P. orbiculare	Mexico: Durango: Otinapa	457	LVT 10768
P. orbiculare	Mexico: Durango: Rancho Las Margaritas	458	LVT 10765
P. orbiculare	Mexico: Estado de Mexico: Jocotitlán	168	LVT 10777

Table 2.1. Collection and voucher data continued.

Taxon	Locality	Sample ID (MX)	Voucher Number
P. orbiculare	Mexico: Estado de Mexico: Huixquilucan	401	LVT 10778
P. orbiculare	Mexico: Estado de Mexico: Villa de Carbon	446	LVT 10772
P. orbiculare	Mexico: Estado de Mexico: Santa Rosa de Lima	449	LVT 10776
P. orbiculare	Mexico: Estado de Mexico: Toluca	451	LVT 10775
P. orbiculare	Mexico: Hidalgo: Mineral del Monte	17	LVT 10780
P. orbiculare	Mexico: Hidalgo: Tulancingo de Bravo	166	LVT 10781
P. orbiculare	Mexico: Hidalgo: Alfajayucan	450	LVT 10783
P. orbiculare	Mexico: Hidalgo: Tenango de Doria	452	LVT 10779
P. orbiculare	Mexico: Jalisco: Vaquerías	162	LVT 10784
P. orbiculare	Mexico: Nayarit: Santa Teresa	336	LVT 10763
P. orbiculare	Mexico: Nuevo León: Pablillo	30	LVT 10790
P. orbiculare	Mexico: Puebla: Tlatlauquitepec	23	LVT 10771
P. orbiculare	Mexico: Queretáro: Amealco	399	LVT 10785
P. orbiculare	Mexico: Queretáro: Amealco	445	LVT 10786
P. orbiculare	Mexico: San Luis Potosí: Guadalcalzar	163	LVT 10788
P. orbiculare	Mexico: San Luis Potosí: Real de Catorce	456	LVT 10793
P. orbiculare	Mexico: Tamaulipas: W Bustamante	204	LVT 10792
P. orbiculare	Mexico: Tamaulipas: SE Bustamante	337	LVT 10789
P. orbiculare	Mexico: Veracruz: Atzompa	20	LVT 10770
P. orbiculare	Mexico: Veracruz: Las Vigas	169	LVT 10769
P. orbiculare	Mexico: Zacatecas: Valparaíso	14	LVT 10764

Table 2.1. Collection and voucher data continued.

Taxon	Locality	Sample ID (MX)	Voucher Number
*P. modestum**	USA: New Mexico: Jornada	--	LVT uncat.
P. douglasii (short-horned clade)*	USA: Idaho: Butte Co.	--	LVT uncat.
P. hernandesi (short-horned clade)*	USA: Nevada: Elko Co.	--	LVT uncat.
P. ditmarsi (short-horned clade)*	Mexico: Sonora	462	TNHC-GDC 8420
*P. asio**	Mexico	460	TNHC-GDC 8305
*P. taurus**	Mexico	461	TNHC-GDC 8540
*P. cornutum**	USA: New Mexico: Doña Ana Co.	463	LVT 374
*P. coronatum**	Mexico: Baja Sur: La Paz	--	LVT 8384
*P. solare**	USA	--	LVT 981
*P. mcalli**	USA:	--	LVT 0971
P. platyrhinos (desert clade)*	USA: Nevada: Nye Co.	--	LVT 9466
P. goodei (desert clade)*	USA:	--	
P. "Yuma" (desert clade)*	USA: Arizona: Yuma Proving Grounds	--	LVT 9951

Table 2.2. Estimated divergence dates within *Phrynosoma orbiculare* based on two molecular clock calibration methods implemented in BEAST. Lineage designations follow Fig. 2. Posterior mean ages followed by 95% highest posterior density intervals in parentheses, provided in millions of years ago.

Divergence event	Fossil-calibrated clock	Rate-calibrated clock
Northern clade / Southern clade	7.7 (5.8–9.7)	7.2 (5.9–8.6)
Northern clade:		
I + II / III + IV + V	6 (4.2–7.8)	5.1 (3.9–6.4)
I / II	3.5 (2–5.1)	3 (2–4)
III / IV + V	2.8 (1.7–3.9)	2.5 (1.8–3.2)
IV / V	1.8 (1–2.6)	1.6 (1.1–2.2)
Southern clade:		
VI / VII + VIII + IX + X + XI	5.4 (3.9–6.9)	5.6 (4.5–6.9)
VII + VIII / IX + X + XI	4.8 (3.5–6.2)	5 (4–6.1)
VII / VIII	2 (1.2–2.8)	2 (1.4–2.7)
IX / X + XI	3.9 (2.6–5.3)	3.8 (2.8–4.9)
X / XI	1.9 (1–2.8)	1.8 (1.1–2.5)

Table 2.3. Comparison of mean estimated divergence dates in *Phrynosoma orbiculare* with co-distributed highland taxa across selected shared barriers within the Mexican highlands. Barriers are shown in Fig. 5. Dates were estimated from mitochondrial gene trees, so for consistency, I did not include slightly younger re-estimates of divergence times in Mexican jays based on a species-tree approach (McCormack et al., 2011).

Barrier	Taxon / Mean divergence date
Rio Mezquital basin	Mexican horned lizards[1] / 1.5 Ma
	Twin-spotted rattlesnakes[2] / 1.2 Ma
	Rock rattlesnakes[3] / 2.4 Ma
Rio Mezquital-Rio Santiago basins	Mexican horned lizards[1] / 2.5 Ma
	Rock rattlesnakes[3] / 1.4 Ma
Rio Culiacán-Rio Nazas basins	Mexican horned lizards[1] / 5.5 Ma
	Twin-spotted rattlesnakes[2] / 2.6 Ma
Cerritos-Arista / Saladan barrier	Mexican horned lizards[1] / 2 Ma
	Rock rattlesnakes[3] / 2.1 Ma
	Mexican jays[4] / 2.4 Ma
	Middle American gophersnakes[5] / 4.5 Ma

[1]this study; [2]Bryson et al., in press; [3]Bryson et al., 2011a; [4]McCormack et al., 2008; [5]Bryson et al., 2011b

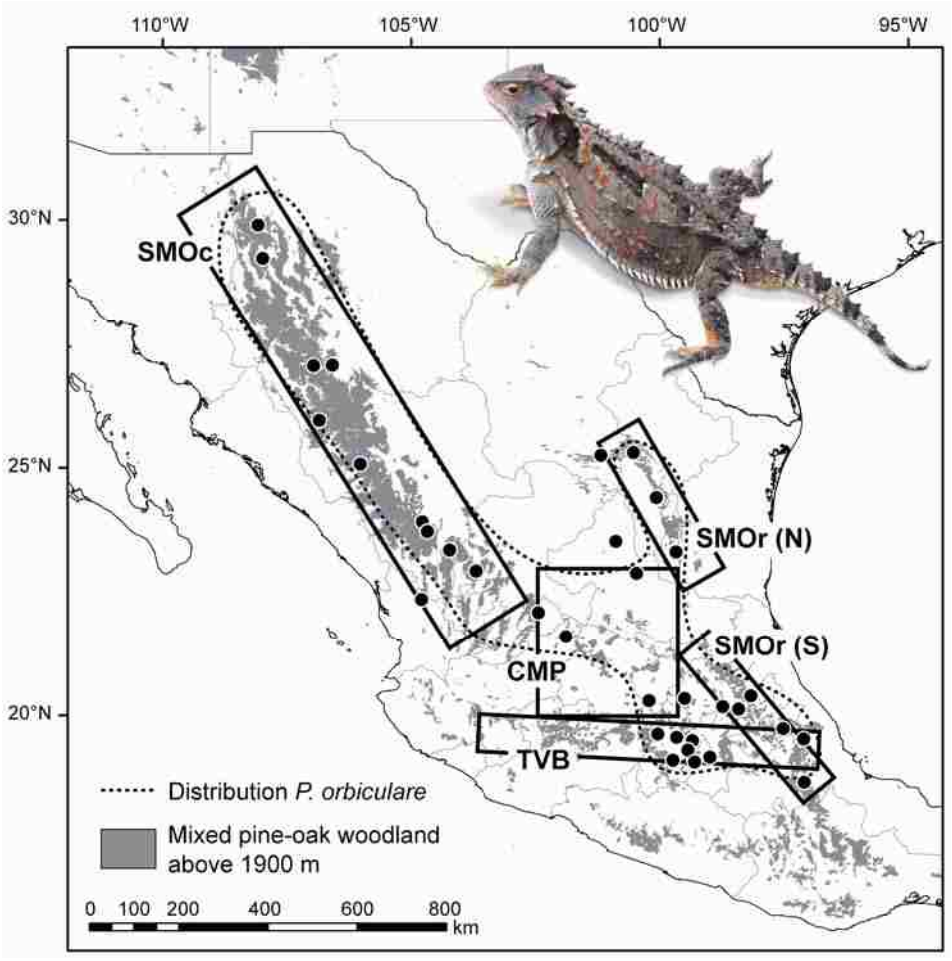

Figure 2.1. Sampling localities for genetic samples of *Phrynosoma orbiculare* overlaid on mixed pine-oak woodlands above 1900 m. Dashed line delineates approximate distribution of *P. orbiculare* (Mendoza-Quijano et al., 2007). Several important mountain ranges in Mexico mentioned in the text include the Sierra Madre Occidental (SMOc), northern (N) and southern (S) Sierra Madre Oriental (SMOr), and Transvolcanic Belt (TVB). The Central Mexican Plateau (CMP) is also noted.

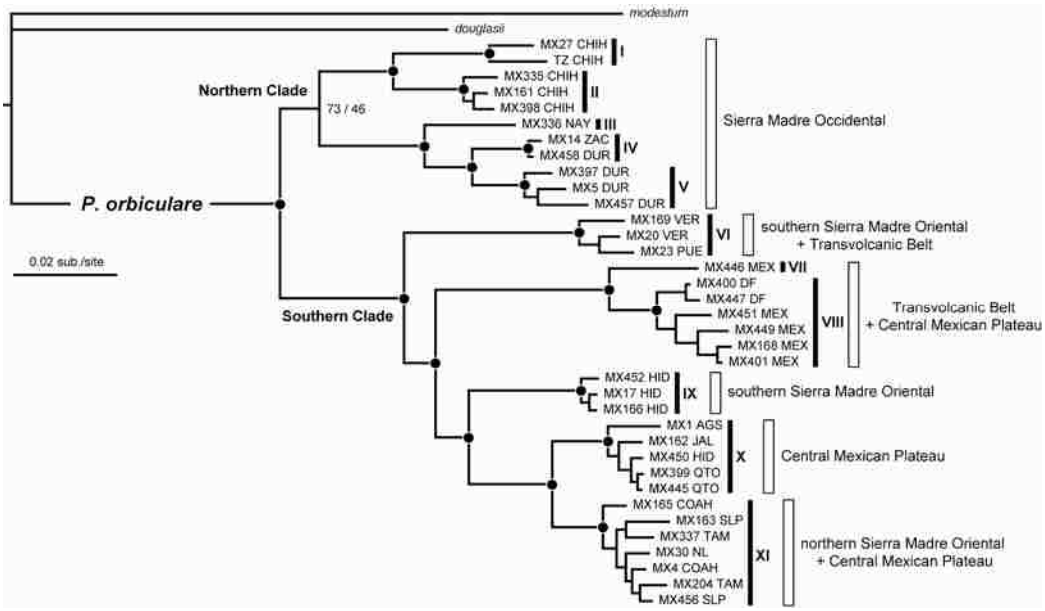

Figure 2.2. Maternal genealogy of *Phrynosoma orbiculare* based on mixed-model Bayesian inference (tree shown) and maximum likelihood analyses of mitochondrial DNA sequence data. Names of two major clades and 11 inferred lineages (denoted with roman numerals) are indicated, and bars show corresponding mountain ranges drawn in Fig. 2.1. Numbers at nodes indicate support values (Bayesian posterior probability followed by maximum likelihood bootstrap). Nodes that received ≥ 95% Bayesian posterior probability and ≥ 70% bootstrap support are depicted with black dots.

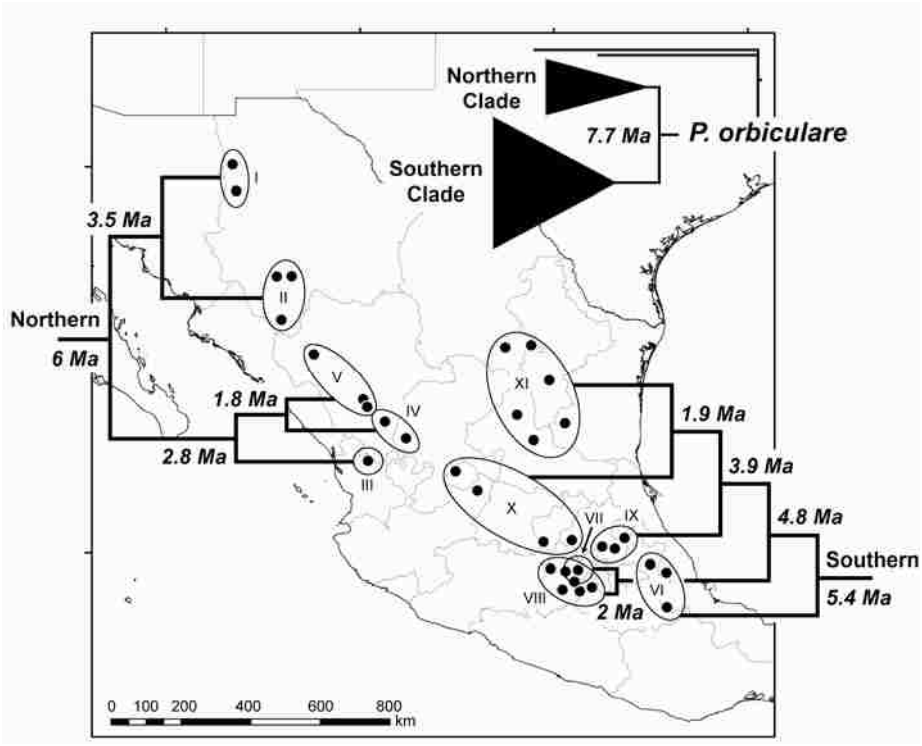

Figure 2.3. Geographic distribution of *Phrynosoma orbiculare* mitochondrial lineages. Roman numerals refer to lineages shown in Fig. 2.2. Numbers at nodes on phylogenetic tree specify approximate estimated divergence times (mean dates derived from fossil-calibrated dataset, see Table 2.2 for credibility intervals and alternative dates based on rate-calibrated analyses)..

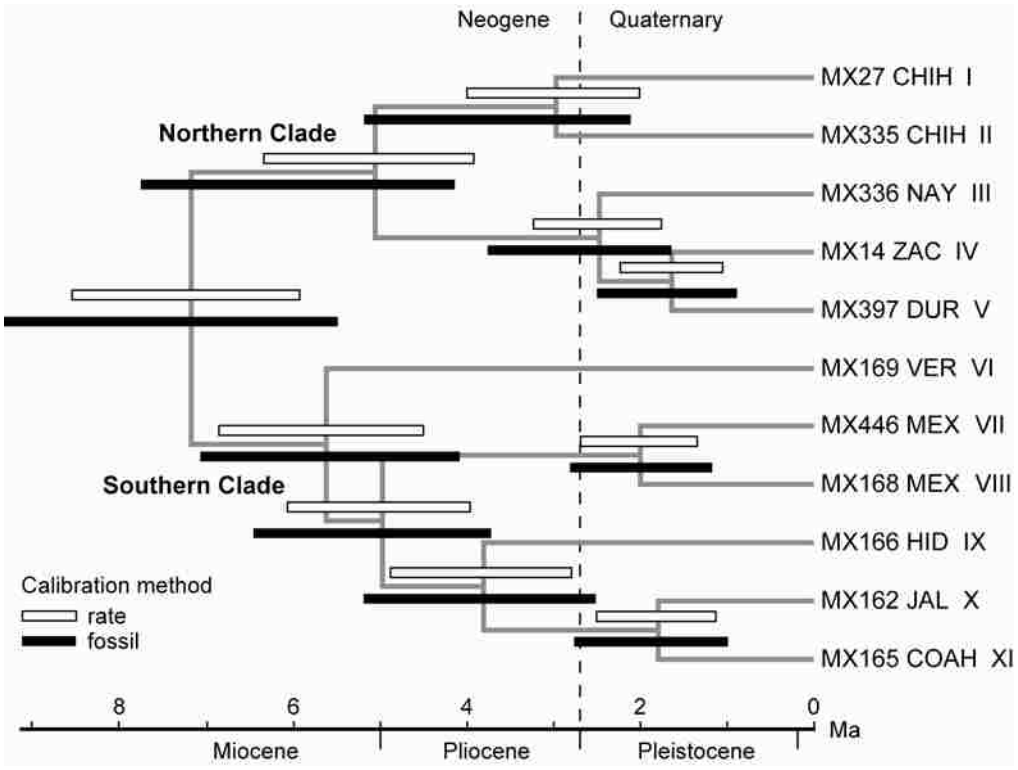

Figure 2.4. Chronogram with estimated divergence times for lineages within *Phrynosoma orbiculare* inferred using Bayesian relaxed clock phylogenetic analyses. Names of two major clades and 11 inferred lineages (denoted with roman numerals) are indicated and follow Fig. 2.2. Bars indicate 95% highest posterior densities derived from fossil-calibrated (black bars) and rate-calibrated (white bars) datasets. Fossil-calibrated tree shown.

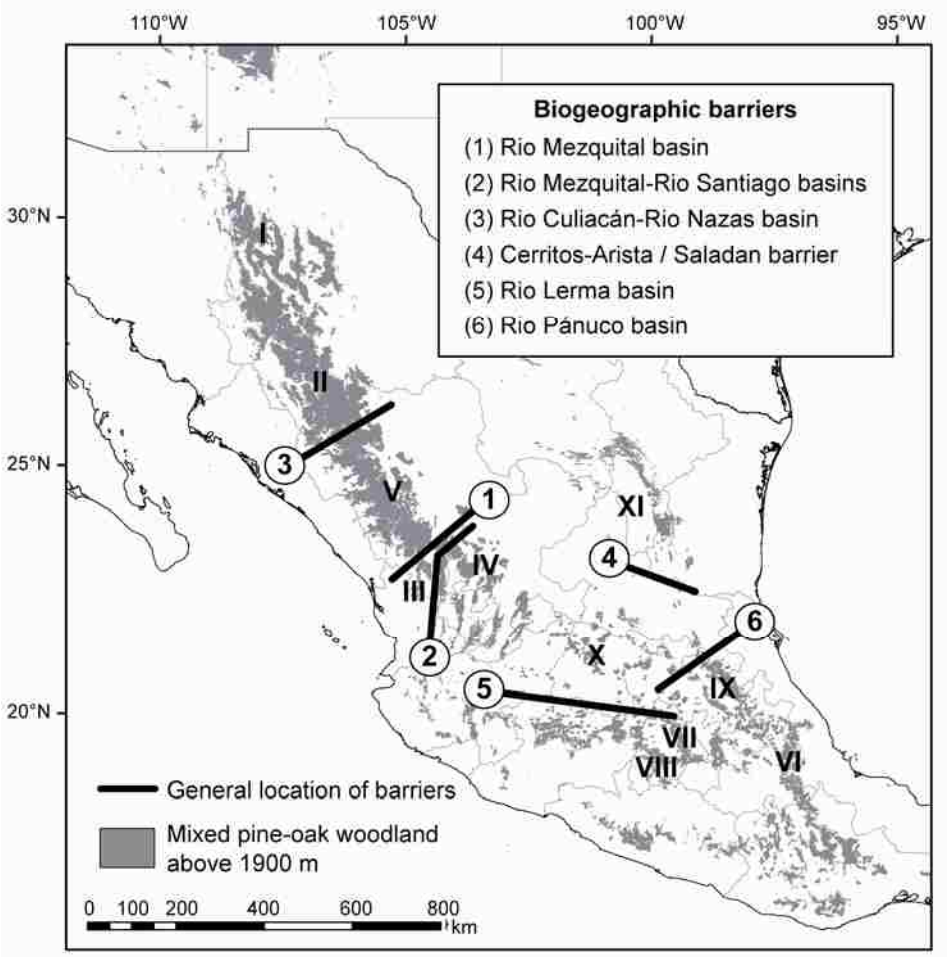

Figure 2.5. Examples of biogeographic barriers shared between *Phrynosoma orbiculare* and co-distributed highland taxa. Roman numerals refer to lineages of *P. orbiculare* delineated in Fig. 2.3, and are placed on the approximate center of distribution of each lineage. Comparison of estimated divergence dates in *P. orbiculare* with co-distributed highland taxa across barriers within the northern sierras (barriers 1–4) listed in Table 2.3.

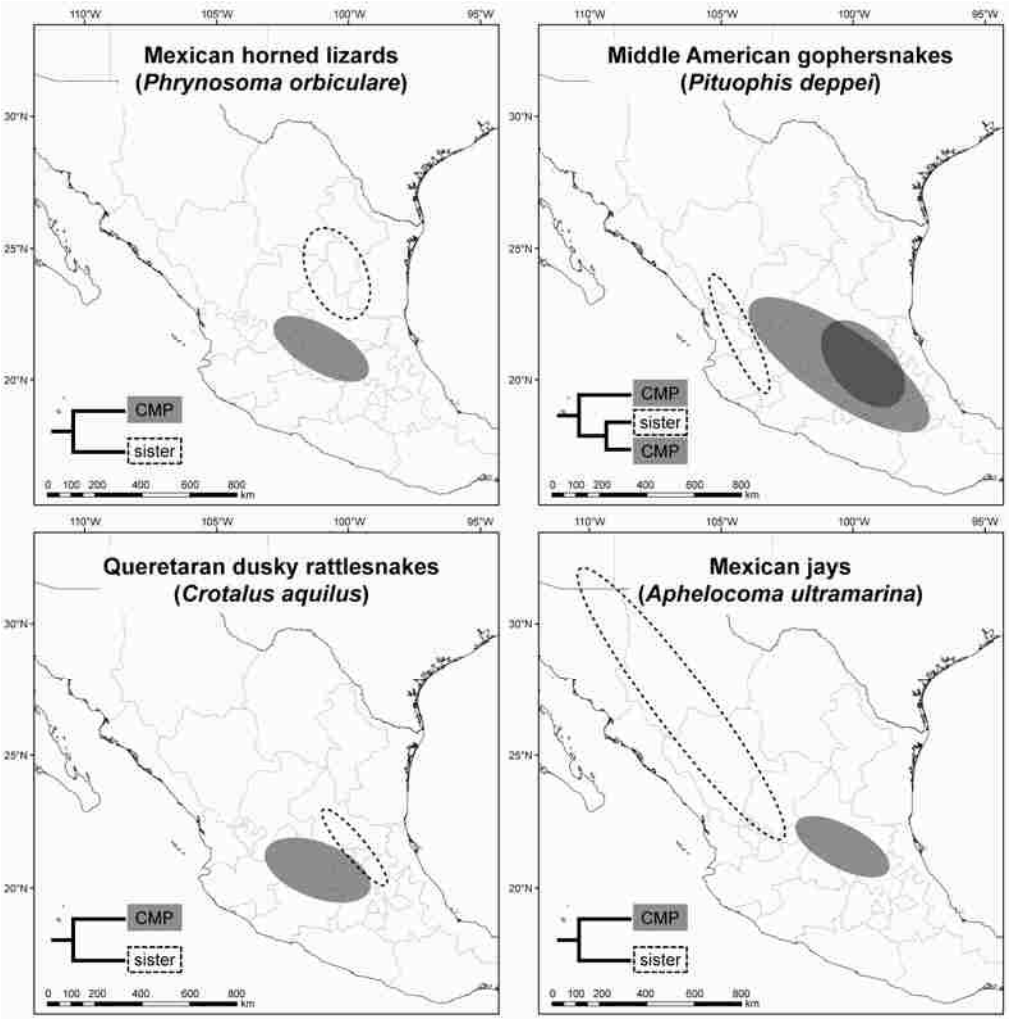

Figure 2.6. Generalized distributions of mitochondrial lineages of highland taxa confined to the Central Mexican Plateau (CMP): Mexican horned lizards (this study), Middle American gophersnakes (Bryson et al., 2011b), Queretaran dusky rattlesnakes (Bryson et al., 2011a), and Mexican jays (McCormack et al., 2008). The approximate distributions of sister lineages are also shown for each taxon to illustrate that the Central Mexican Plateau is accumulating lineages from geographically different sources.

CHAPTER 3

TESTING THE ROLES OF NEOGENE VICARIANCE AND QUATERNARY CLIMATE CHANGE ON THE HISTORICAL DIVERSIFICATION OF BUNCHGRASS LIZARDS (*SCELOPORUS SCALARIS* GROUP)

Introduction

Emerging patterns of historical diversification in the Mexican highlands suggest mixed responses in co-distributed taxa to past geological and climatic events despite a presumed shared history in the same region (Sullivan et al., 2000; Paniagua and Morrone, 2009; Bryson et al., 2011b). Vicariance in the Miocene and Pliocene heavily influenced lineage divergences in some taxa (e.g., Castoe et al., 2009), while Quaternary climate change triggered increased diversification in others (e.g., Bryson et al., in press). The synergistic effects of Earth history and glacial-interglacial cycles, coupled with the complex topography of Mexico, appear to have produced a myriad of species-specific responses. Reconciling a common pattern of lineage diversification in Mexican highland taxa has proven difficult (Flores-Villela and Martínez-Salazar, 2009)

Ancient development over 30 million years ago (Ma) of most of the major mountains in Mexico (Ferrusquía-Villafranca and González-Guzmán, 2005) probably pre-dates diversification of the extant highland-adapted species. Neogene formation of the Transvolcanic Belt (TVB), however, undoubtedly affected both the timing and tempo of diversification in many montane species. This volcanic chain of mountains is one of the predominant geographical features of Mexico, and its geological development has been posited as a primary contributor to the biogeographic histories of numerous taxa (Mulcahy et al., 2006; Bryson et al., 2011a). Uplift of the TVB created new geographical

barriers and montane habitats, but also linked previously isolated highland biotas (Anducho-Reyes et al., 2008). The complex geological history of this mountain range (Ferrusquía-Villafranca, 1993; Gómez-Tuena et al., 2007) unfortunately makes accurate dating of vicariant events presumably responsible for divergences among co-distributed taxa difficult. A recent revision of the past two decades of research on the origin of the TVB (Gómez-Tuena et al., 2007) suggests four major volcanic episodes during the Neogene formed most of the range. Two of these episodes (Fig. 1), one at around 10–19 Ma and one about 3–7.5 Ma, resulted in major mountain formations that almost completely subdivided Mexico. Estimated mean divergence dates in several taxa distributed on or near this region are largely congruent with these two periods (Table 1). In particular, numerous divergences are remarkably similar at around 4–7 Ma. These dates suggest that the marked period of uplift around 3–7.5 Ma may have had a comparatively stronger effect on lineage diversification than other periods of uplift.

In addition to Neogene vicariant events, Pleistocene climate change is expected to have an effect on biotic diversification across the Mexican highlands. Highland biotas were repeatedly fragmented during warm interglacial periods as pine-oak woodlands retracted to higher, cooler elevations (McDonald, 1993; Metcalfe et al., 2000; Gugger et al., 2011). Diversification in several highland taxa appears linked to Pleistocene climate change (León-Panigua et al., 2007; Ruiz et al., 2010; Bryson et al., in press). The signal of Pleistocene divergence is likely to be particularly evident as amplitude and duration of glacial cycles increased during the mid-Pleistocene pluvial–interpluvial period beginning 0.9 Ma (Webb and Bartlein, 1992; Hewitt, 2000). Globally, these glacial processes impacted diversification in a number of organisms (Hewitt, 1996, 2000).

Bunchgrass lizards in the *Sceloporus scalaris* group provide an attractive study system to test influences of Neogene vicariance and Pleistocene climate change on the timing and tempo of lineage diversification across the Mexican highlands. Members of the *S. scalaris* group are widely distributed across montane grasslands associated with mixed pine-oak forests along the Sierra Madre Occidental, Sierra Madre Oriental, and TVB (Smith et al., 1993; Smith et al., 1996; Watkins-Colwell et al., 2006; Figs. 2–3). They occur on all sides of the TVB, so a diversification hypothesis invoking the uplift of this range can be tested. The *S. scalaris* group includes six monotypic species, *S. slevini*, *S. samcolemani*, *S. chaneyi*, *S. goldmani*, and *S. bicanthalis*, and two polytypic species, *S. scalaris* (*S. s. scalaris*, *S. s. unicanthalis*, *S. s. brownorum*) and *S. aeneus* (S. *a. aeneus*, *S. a. subniger*) (Smith et al. 1993; Watkins-Colwell et al., 2006).

In this study, I investigated the relative roles of Neogene vicariance and Quaternary climate change on lineage diversification in the *S. scalaris* group. I combined extensive range-wide sampling and mixed-model phylogenetic analyses of mitochondrial DNA (mtDNA) to formulate a robust hypothesis of matrilineal relationships. Concerns regarding the use of mtDNA gene estimates in analyses have been raised (e.g., Edwards and Bensch, 2009), yet this marker appears useful for detecting recent geographic patterns (Moore, 1995; Hudson and Coyne, 2002; Zink and Barrowclough, 2008; Barrowclough and Zink, 2009) and can lead to significant biogeographic discoveries (e.g., Upton and Murphy, 1997; Riddle et al., 2000a). Molecular dating using mtDNA gene trees is also of concern since gene trees may overestimate divergence times (Jennings and Edwards, 2005; Burbrink and Pyron, 2011; Kubatko et al., 2011). However, overestimation may become less of an issue at deeper time scales (Edwards

and Beerli, 2000), and some gene splits may better reflect the history of initial divergences (McCormack et al., 2008). To provide a temporal component to my matrilineal phylogeny of the *S. scalaris* group, I estimated dates of lineage divergences based on a relaxed molecular clock. I then tested the hypothesis of a diversification rate shift in response to a period of TVB uplifting 3–7.5 Ma against the null hypothesis of no diversification rate shift. I also investigated the impact of mid-Pleistocene climate oscillations on diversification within the *S. scalaris* group. Results provided insight into the emerging evolution of Mexican highland biota and the impacts of Neogene vicariance and climate change on lineage diversification.

Methods

Taxon sampling and laboratory methods

I obtained tissues from 72 *S. scalaris* group species (Table 2) from across their distributions (Figs. 2–3). Taxonomic designations were made on the basis of male coloration, parity mode, and distribution maps (Smith et al., 1993; Smith et al., 1996; Watkins-Colwell et al., 2006). *Sceloporus a. aeneus* and *S. a. subniger* have recently been considered subspecies (Smith et al., 1993), full species (i.e., *S. aeneus* and *S. subniger*) (Wiens and Reeder, 1997; Wiens et al., 2010), or a single species (*S. aeneus*) (Benabib et al., 1997). I conservatively treated each as subspecies. I sampled three known localities of *S. goldmani* in Coahuila (Lemos-Espinal and Smith, 2007), but failed to find this species. At two localities (Sierra La Concordia and west of San Antonio de las Alazanas), I found only *S. samcolemani*. The third site near Goméz Farías was severely

degraded desert grassland, and no *S. scalaris* group lizards were seen. *Sceloporus goldmani* may be extinct at lower elevations (Sinervo et al., 2010). I also failed to find *S. a. subniger* in northwestern Guanajuato. It has been suggested that this species has been locally extirpated in this region (Mendoza-Quijano et al., 2001). I added partial gene sequences for 3 samples from GenBank to fill in sampling gaps (Table 2). I used *S. graciosus* and *S. undulatus* as outgroups based on previous phylogenetic studies (Wiens and Reeder, 1997; Wiens et al., 2010).

I sequenced two mtDNA gene regions, including NADH dehydrogenase subunit 4 and flanking tRNAs (ND4) and ATPase subunits 8 and 6 (ATPase 8, ATPase 6). These gene regions have been previously shown to be informative at different levels of divergence within lizards (Leaché and Mulcahy, 2007; Lindell et al., 2008). Total genomic DNA was extracted from liver or tail clips using the QIAGEN DNeasy Blood and Tissue Kit (Qiagen, Valencia, CA) following manufacturer's recommendations. All gene regions were amplified via PCR in a mix containing 6.25 µl Takara ExTaq Polymerase Premix (Takara Mirus Bio Inc., Madison, WI, USA), 4.25 µl double-distilled water, 0.5 µl each primer (10 µl), and 1.0 µl of template DNA. Primer sequences for ND4 are given in Arévalo et al. (1994), and for ATPase were specifically designed for this project (C2LF, 5'– ATCTGCGGGTCAAACCACAG–3'; C3LR, 5'– GCGTGTGYTTGGTGGGTCAT–3'). DNA was denatured initially at 95 °C for 2.5 min; 35–40 cycles of amplification were then performed under the following conditions: denaturation at 95 °C for 1 min, annealing at 56 °C for 1 min, and extension at 72 °C for 1 min; this was followed by a final 10 min elongation at 72 °C. Double-stranded PCR amplified products were checked by electrophoresis on a 1% agarose gel, purified using

exonuclease and shrimp phosphatase, and directly sequenced in both directions with the amplification primers using a Big Dye Terminator v. 3.1 cycle sequencing kit (Applied Biosystems, Foster City, CA, USA). The completed sequencing reactions were cleaned of excess dyes using CentriSep spin columns (Princeton Separations, Inc., Adelphia, NJ), and sequences were visualized on an ABI Prism 3130 capillary autosequencer. Forward and reverse sequences for each individual were edited and manually aligned using Sequencher 4.2 (Gene Codes Corporation, Ann Arbor, MI).

Phylogenetic analyses

I analyzed my sequence data using Bayesian inference (BI) and maximum likelihood (ML) phylogenetic methods. Bayesian inference analyses were conducted using MrBayes 3.1 (Ronquist and Huelsenbeck, 2003) on the combined mtDNA dataset, implementing separate models for each gene region (ND4, tRNAs, ATPase 8, ATPase 6). For the three GenBank samples (Table 2), only available ND4 and associated tRNAs sequence data were included in analyses. MrModeltest 2.1 (Nylander, 2004) was used to select a best-fit model of evolution, based on Akaike Information Criteria (AIC), for each partition. Bayesian settings included random starting trees, a variable rate prior, a mean branch length exponential prior of 100, and heating temperature of 0.04. Analyses consisted of four runs (nruns=4) conducted each with three heated and one cold Markov chain sampling every 100 generations for 4 million generations. Output parameters were visualized using the program TRACER v1.4 (Rambaut and Drummond, 2007) to ascertain stationarity and whether the duplicated runs had converged on the same mean likelihood. Convergence was further assessed using AWTY (Nylander et al., 2008). After determining chain convergence, which occurred during the first 500,000 generations of

each run, I conservatively discarded all samples obtained during the first one million (25%) generations as burn-in. A 50% majority-rule consensus phylogram with nodal posterior probability support was estimated from the combination of the four runs post-burn-in. Maximum likelihood analyses were conducted using RAxML 7.0.3 (Stamatakis, 2006) with the same partitioning scheme used for the BI analyses. The GTRGAMMA model was used, and 1000 nonparametric bootstrap replicates were performed to assess nodal support. I considered those nodes with ≥ 95% Bayesian posterior probability and ≥ 70% bootstrap support as strongly supported (Hillis and Bull, 1993; Felsenstein, 2004).

Divergence dating

Divergence dates were estimated using a Bayesian molecular clock framework implemented in the program BEAST v1.6.1 (Drummond and Rambaut, 2007). Two different methods for estimating divergence times were used. Divergence estimates were inferred for a reduced dataset, which included one individual from each geographically structured lineage. The first method utilized a relaxed uncorrelated lognormal clock and node constraints obtained from the fossil record. To calibrate the tree, I included sequences from several outgroups (Table 3). The second method employed a substitution rate calibration and relaxed uncorrelated lognormal clock. I used a mtDNA rate calibration previously calculated from a similar sized lizard (Macey et al., 1999). This substitution rate, here corrected to 8.05×10^{-3} substitutions/site/million year using a more complex GTR + G model, has been used in a number of studies to date divergences in lizards (e.g., Morando et al., 2004; Tennesson and Zamudio, 2008; Luxbacher and Knouft, 2009). For both datasets, best-fit models of evolution were re-estimated using MrModeltest, and unlinked across partitions.

For each method, analyses consisted of two independent runs each of 40 million generations, with samples retained every 1000 generations, and with a Yule tree prior. Results were displayed in TRACER to confirm acceptable mixing and likelihood stationarity, appropriate burn-in, and adequate effective sample sizes. After discarding the first 4 million generations (10%) as burn-in, the trees and parameter estimates from the two runs were combined using LogCombiner v1.6.1 (Drummond and Rambaut, 2007). The parameter values of the samples from the posterior distribution were summarized on the maximum clade credibility tree using TreeAnnotator v1.6.1 (Drummond and Rambaut, 2007), with the posterior probability limit set to zero and mean node heights summarized.

For calibrated analyses, three fossil constraints taken from the paleoherpetological literature were used: (1) the oldest known fossils referable to *Sceloporus* from the Early Miocene (Arikareean North American Land Mammal Age (NALMA); Robinson and Van Devender, 1973; Yatkola, 1976; Holman, 1970, 1995), (2) the oldest known fossils referable to *S. jarrovii* from the Middle Miocene (Hemingfordian NALMA; Yatkola, 1976; Estes, 1983), and (3) the oldest known fossil of *S. undulatus* from the Pliocene (Blancan NALMA; Rogers, 1976; Estes, 1983). The stem of *Sceloporus* was constrained with a zero offset (hard upper bound) of 20 Ma, a lognormal mean of 0.7, and a lognormal standard deviation of 1.0. This produced a median age of 22 Ma and a 95% prior credible interval (PCI) extending to the end of the Arikareean 30 Ma. The stem of the *S. jarrovii* clade (Table 3) was constrained with a zero offset of 16 Ma representing the end of the Hemingfordian, a lognormal mean of 0.7, and a lognormal standard deviation of 0.5. This produced a median age of 18 Ma and a 95% PCI extending to the

end of the Hemingfordian 20 Ma. The node representing the most recent common ancestor (MRCA) of the *S. undulatus* clade (Table 3) was constrained with a zero offset of 1.8 Ma (the end of the Blancan), a lognormal mean of 0.1, and a lognormal standard deviation of 0.65. This produced a median age of 3 Ma and a 95% prior credible interval (PCI) extending to the end of the Blancan 5 Ma. These lognormal distributions with hard lower bounds best reflect the prediction, based on the high likelihood of fossil non-preservation, that any true divergence date will probably be older than the oldest known fossil, rather than younger (Ho and Phillips, 2009; Kelly et al., 2009).

Tests of differential diversification rates

I employed two methodological approaches to test for differential diversification rates across the *S. scalaris* group mtDNA phylogeny in response to uplifting of the TVB and climate oscillations beginning with the mid-Pleistocene shift in duration of glacial – interglacial cycles. The first method compared inferred topological distribution to a random distribution to determine if diversification rate shifted across the tree. My second approach compared the temporal distribution of inferred divergence events to a randomly created distribution to test when and where shifts in diversification took place along my phylogeny. If Neogene uplifting of the TVB affected diversification rates in the *S. scalaris* group, then diversification rates should shift near the root of the clade or clades containing TVB species (*S. aeneus*, *S. bicanthalis*). If rate shifts are associated with one of the major volcanic episodes that occurred 3–7.5 Ma, then most divergences should have happened during this time period. Likewise, if mid-Pleistocene climate change affected diversification rates, then rates should shift near the tips of the phylogeny during the start of extreme glacial periods 0.9 Ma.

The program SYMMETREE v1.1 (Chan and Moore, 2005) and was used to test the general hypothesis of variation in diversification rates across the *S. scalaris* group mtDNA phylogeny. The batch processing option was applied using the posterior probability distribution of 1000 post burn-in trees generated from the rate-calibrated BEAST analyses. Trees from the posterior distribution of my fossil-calibrated BEAST analyses were not selected since I lacked complete sampling of the entire *Sceloporus* species tree (Wiens et al., 2010), which could bias results (Moore and Chan, 2007). Removing the outgroups would require manually pruning 1000 post burn-in trees. I used a taxon-size sensitive (TSS) equal-rates Markov (ERM) branching model to resolve polytomies. Equal-rates Markov models assume that each terminal in an expanding tree has an equal and independent probability of splitting and uses a random taxon-addition approach to resolve polytomies. The number of random resolutions was set to 10 000 whole trees. To calculate *P*-values for the tree statistics implemented in SYMMETREE, I generated a null distribution of 1 million simulated trees with the same number of species as the observed trees under the ERM model. Likelihood ratio-based delta statistics were estimated to locate diversification rate shifts in certain areas of the phylogeny, if present. SYMMETREE does not provide a batch-summary block for the shift statistics, so *P*-value ranges were visually inspected in output blocks.

I analyzed temporal shifts in diversification rates using ML-based diversification-rate analysis (Rabosky, 2006a). Divergence dates estimated from both calibration methods in BEAST were used. The fit of different birth–death models implementing two constant rates (pure-birth, and birth–death) and four variable rates (exponential and logistic density-dependent, and two-rate and three-rate pure-birth) was computed with

LASER 2.3 (Rabosky, 2006b). Model fit was measured using AIC scores. Significance of the change in AIC scores (ΔAICrc) between the best rate-constant and best rate-variable model was determined by creating a null distribution for ΔAICrc. This was done by simulating 1000 trees using yuleSim in LASER with the same number of nodes and the same speciation rate as that estimated under the pure-birth model. I additionally generated a lineage-through-time (LTT) plot using the plotLtt function in LASER to visualize the pattern of accumulation of log-lineages over time.

Results

Sequence characteristics and phylogenetic estimate

The final dataset consisted of 1698 aligned nucleotide positions. Models of sequence evolution selected for the partitions were GTR + I + G (ND4, ATPase 8, ATPase 6), and HKY + I + G (tRNA). All sequences were deposited in GenBank.

Within the *S. scalaris* group, I identified two major mtDNA clades that contained 13 strongly supported lineages (Figs. 5–6). One clade contained samples from the two major sierras of northern Mexico ('northern clade'). Samples geographically proximate to the TVB grouped together with samples from the Central Mexican Plateau in a 'southern clade'. Four lineages within these clades corresponded to the species *S. chaneyi*, *S. samcolemani*, *S. slevini*, and *S. bicanthalis*. Three lineages represented the subspecies *S. s. scalaris*, *S. s. unicanthalis*, and *S. s. brownorum*. The species *S. aeneus* appeared to be a composite of four distinct lineages, none of which uniquely encompassed the two subspecies *S. a. aeneus* and *S. a. subniger*. These four lineages were geographically

structured, and labeled '*aeneus* West', '*aeneus* Central', '*aeneus* East', and '*aeneus* South'. Two lineages represented undescribed taxa, one previously assigned to *S. s. brownorum* from Aguascalientes (Smith et al., 1997), and one previously considered *S. s. scalaris* from Tapalpa, Jalisco (Watkins-Colwell et al., 1996). Additional geographic structure was present within *S. slevini*, *S. samcolemani*, and *S. bicanthalis* (Fig. 4).

Relationships among lineages within the southern clade were in general difficult to infer. Collapsing the weakly supported *S. bicanthalis* + *aeneus* West sister relationship formed a large basal polytomy of four lineages and two smaller clades (*aeneus* South + *aeneus* Central / *S. s. scalaris*, and Aguascalientes + *S. s. unicanthalis*). In the northern clade, the two Sierra Madre Oriental lineages *S. chaneyi* and *S. samcolemani* were sister, and the two Sierra Madre Occidental lineages *S. slevini* and *S. s. brownorum* were sister. Together these two mountains formed a strongly supported sister relationship.

Divergence dating

The selected models of sequence evolution for the fossil-calibrated and rate-calibrated datasets in the BEAST analyses were GTR + I + G (ND4, ATP8, ATP6), HKY + I + G (tRNA, fossil-calibrated), and HKY + I (tRNA, rate-calibrated). Estimated dates of divergences using both methods of clock calibration differed (Fig. 6). Based on the fossil-calibrated analyses, mean substitution rate within the *S. scalaris* group more closely approached 1.2×10^{-2} substitutions/site/million year (2.4% between lineages per million years), which is much faster than the rate I used for rate-calibrated analyses (1.61% between lineages per million years). Additionally, the branching order in each maximum clade credibility tree (Fig. 6) differed as a result of rearrangements of several weakly supported nodes. Despite these differences, the majority of divergences estimated

by both methods appear to predate the pluvial-interpluvial period of the mid-Pleistocene (Fig. 6). In the southern clade, mean divergence dates fell largely within an episode of TVB volcanism 3–7.5 Ma.

Tests of differential diversification rates

Results from batch analyses in SYMMETREE indicate no significant variation in diversification rate in the *S. scalaris* group topology. Examination of delta statistics for individual trees, however, reveal numerous significant (P=0.05) diversification rate shifts along the branch leading to the southern clade of the *S. scalaris* group. This clade contains all lineages associated with the TVB.

Birth–death likelihood analyses rejected the null hypothesis of rate-constancy for both datasets (P=0.001 fossil-calibrated, P=0.005 rate-calibrated). The rate-variable model that best fit each dataset differed (Table 4). For the fossil-calibrated dataset, the logistic density-dependent (DDL) model provided a better fit. Under this model, diversification rate in the *S. scalaris* group has gradually decreased through time, with diversification rate estimated at 0.73 divergences per million years. The three-rate birth-death (Yule3) model provided the best fit to the rate-calibrated dataset. According to the scenario suggested by this model (Fig. 6), net diversification rate in the *S. scalaris* group increased dramatically at 6.8 Ma from 0.1 to 0.42 divergences per million years, then decreased at 4 Ma to 0.03. These shifts correspond well with predicted diversification rate changes associated with uplifting of the TVB 3–7.5 Ma.

It is worth noting that alternative rate-variable models may also be a good fit to the data (Table 4). For the fossil-calibrated dataset, the best-fit DDL model differs in AIC from the next best-fit rate-variable model, Yule3, by a value of only 0.98. Here, net

diversification rate increased at about 5.5 Ma and decreased at 2.8 Ma (Fig. 6). Much of this period falls within the predicted range of TVB uplifting. Diversification rate was initially 0.08 divergences per million years, increased to 0.5, then declined to 0.04. For the rate-calibrated dataset, a Yule2 rate-variable model differs in AIC score from the best-fit Yule3 model by 0.65. This Yule2 model predicts a single decrease in diversification rate at 4 Ma (Fig. 6), from an initial rate of 0.28 divergences per million years to 0.03.

Discussion

The Transvolcanic Belt as an emerging driver of lineage diversification

Neogene vicariance appears to be the primary driver of lineage diversification in the *S. scalaris* group. Divergences were temporally and geographically congruent with distinct periods of uplift across the TVB. The earliest divergence between the northern and southern clades around the Middle to Late Miocene (Fig. 6) coincide with the first major TVB volcanic episode 10–19 Ma (Gómez-Tuena et al., 2007). Diversification rate appears to have then shifted around 4–7 Ma. This time period is largely coincidental with a second marked period of volcanism along the TVB 3–7.5 Ma (Rosas-Elguera et al., 2003; Gómez-Tuena et al., 2007; Fig. 1). Diversification rate changes may have been driven by rapid divergences between lineages along the TVB, as indicated by my topological analyses.

Accumulating evidence posits uplifting of the TVB as an emergent and testable driver of diversification in highland taxa. Despite the complex nature of orogenesis

(Ferrusquía-Villafranca, 1993; Gómez-Tuena et al., 2007), most mean lineage divergence dates in the *S. scalaris* group and co-distributed taxa associated with the TVB fall within 4–7 Ma. Exceptions among lowland taxa at the western edge of the TVB that split around 8–16 Ma (Mateos et al., 2002), 9.6 Ma (Devitt, 2006), and 13 Ma (Bryson et al., 2010) paired with my estimated basal split in the *S. scalaris* group during this same time frame suggest the initial volcanic episode across the TVB approximately 10–19 Ma may also be an important driver of lineage diversification. Future studies of highland Mexican taxa with distributions spanning the TVB should test for a causative link between diversification and uplift of the TVB. Two main episodes of volcanic uplift, in particular one that occurred about 3–7.5 Ma, appear to have strong roles in driving lineage diversification across the TVB.

Neogene diversification in northern Mexico

While diversification in the *S. scalaris* group was centered around the TVB, several other Neogene divergences appeared to have occurred in northern Mexico. Most notable is an inferred Middle to Late Miocene divergence between Sierra Madre Occidental and Sierra Madre Oriental lineages (Fig. 6). While a close biotic relationship has been inferred between these two mountain ranges (Marshall and Liebherr, 2000), my estimated dates of divergence far predate the Pleistocene when the highland biota of the Sierra Madre Occidental and Sierra Madre Oriental were probably connected by a continuous corridor of montane vegetation (Gugger et al., 2010; Bryson et al., in press). Rather, my estimated divergence dates more closely approximate inferred Neogene splits in other taxa (Mexican jays, McCormack et al., 2008, 2011; alligator lizards, Zaldivar-Riverón et al., 2005).

Several geographically structured maternal groups are embedded within the Sierra Madre Occidental and northern Sierra Madre Oriental (Fig. 5). Interestingly, several co-distributed highland species show similar fine-scale geographic subdivisions within these mountain ranges (Gugger et al., 2010; Bryson et al., 2011a; Bryson et al., in review). However, estimated dates of divergences between embedded lineages in these studies vary, and range from Miocene to Pleistocene. This suggests that deep canyons that bisect these mountains and low elevation xeric habitats (Fig. 3) may be acting as overlooked filter barriers that promote diversification through time (Wiens, 2004).

Quaternary impacts on lineage diversification

Quaternary climate change appears to have had little effect on lineage diversification in the *S. scalaris* group. Nearly all divergences within the group predate the major pluvial-interpluvial cycles beginning around 0.9 Ma in the mid-Pleistocene (Fig. 6). Depending on the method of molecular clock calibration I used, few mean estimated divergences fell within the Pleistocene (Fig. 6). This finding suggests most lineages in the *S. scalaris* group might be the products of pre-Quaternary fragmentation. Diversification may have occurred in concert with Neogene orogeny and the expansion of C4 grasslands (Neiswenter and Riddle, 2010), and Pleistocene connectivity of previously fragmented highland biotas (Gugger et al., 2010; Bryson et al., in press) did not erase Neogene genetic footprints. The *S. scalaris* group may thus be unique among similar co-distributed highland taxa with widespread distributions in Mexico that show varying degrees of Pleistocene diversification (Zaldivar-Riverón et al., 2005; Moreno-Letelier and Pinero, 2009; Gugger et al., 2010; Bryson et al., 2011a; Bryson et al., 2011b; McCormack et al., 2011; Bryson et al., in press).

Recent studies (Burbrink and Pyron, 2011; Kubatko et al., 2011; McCormack et al., 2011) have provided evidence that divergence times can be significantly overestimated using gene-tree based approaches such as ours that do not correct for genetic divergences that predate speciation. Multilocus species-tree approaches that incorporate coalescent stochasticity generally estimate more recent times of divergences. If this is true, then many of the relatively ancient inferred divergences in the *S. scalaris* group may actually be much younger, placing more divergences within the Pleistocene. However, mtDNA might better reflect the history of initial divergence, especially if nuclear gene flow across lineage boundaries erases or obscures nuclear gene divergences (McCormack et al., 2011). Future studies should incorporate multilocus data and coalescent species-tree models to re-evaluate my divergence estimates. Comparisons of divergence dates in co-distributed taxa across shared biogeographic barriers should then be made based on species tree estimates rather than gene tree estimates.

Conclusions

The *S. scalaris* group has proven useful for studying the impacts of Neogene vicariance and Quaternary climate change on diversification in a wide-ranging highland organism. My results have broad implications for understanding impacts of shared historical events on co-distributed species. Uplift of the Transvolcanic Belt is an emergent and testable driver of lineage diversification. At least one episode of widespread volcanism in the Late Miocene and Pliocene heavily impacted highland taxa. Extreme climatic oscillations in the Pleistocene, a key driver of lineage diversification in some taxa (León-Paniagua et al., 2007; Ruiz et al., 2010; Bryson et al., in press), did not substantially affect diversification rates in all Mexican highland species.

The Mexican highlands are considered one of the world's great biodiversity hotspots (Mittermeier et al., 2005), yet our understanding of the evolutionary drivers generating this diversity remains fragmentary (McCormack et al., 2008; Bryson et al., 2011a). Diversification in the *S. scalaris* group is a good example of how the complex dynamics between past geological and climatic events work together to shape biodiversity. The addition of future studies linking genetic diversity of Mexican highland taxa with their paleohistories will provide further insight into the historical processes responsible for diversification in this complex system.

Table 3.1. Mean estimated divergence dates in several taxa distributed across the Transvolcanic Belt. Posterior mean ages followed by 95% confidence or highest posterior density intervals in parentheses, provided in millions of years ago. Dates were estimated from mitochondrial gene trees, so for consistency, I did not include slightly younger re-estimates of divergence times in Mexican jays based on a species-tree approach (McCormack et al., 2011).

Taxon	Estimated divergence dates (Ma)	Source
Canyon treefrog (*Hyla arenicolor*)	13.5 (6.2–21.7)	Bryson et al., 2010
Western lyresnakes (*Trimorphodon biscutatus*)	9.6 (7.2–13.1)	Devitt, 2006
Topminnows (*Poeciliopsis* subgenus)	8–16	Mateos et al., 2002
Heroine cichlids (*Herichthys* + multiple other species)	6.7 (4.7–8.7)	Hulsey et al., 2004
Middle American gophersnakes (*Pituophis*)	6.7 (5–8.6)	Bryson et al., 2011b
Dusky rattlesnakes (*Crotalus triseriatus* group)	6.3 (5–7.9), 5.4 (4.3–6.8), 4.9 (3.8–6.1)	Bryson et al., 2011a
Mexican jays (*Aphelocoma ultramarina*)	5.6 (4.4–9.4)	McCormack et al., 2008
Gulf Coast toads (*Ollotis valliceps* species group)	5.4 (4.2–7.6)	Mulcahy and Mendelson, 2000
Small-headed rattlesnakes (*Crotalus intermedius* group)	5.2 (3.7–6.9)	Bryson et al., in press
Topminnows (*Poeciliopsis* subclades)	5.1 (4.4–5.8), 3.8 (3.3–4.5)	Mateos, 2005
Molly (*Poecilia butleri*)	4.4 (2.44–6.36)	Mateos, 2005

Table 3.2. Collection and voucher data for *Sceloporus scalaris* samples used in this study. All samples deposited in the Las Vegas Tissue Collection (LVT), Ambrose Monell Cryo Collection (AMCC), Louisiana State University Museum of Natural Science (LSUMNS), or Museum of Vertebrate Zoology, University of California, Berkeley (MVZ).

Sample ID (MX)	Taxon	Locality	Voucher Number
3	*S. a. subniger*	Mexico: Estado de Mexico: Atlacomulco	LVT 10689
7	*S. s. scalaris*	Mexico: San Luis Potosí: Guadalcalzar	LVT 10690
10	*S. s. brownorum*	Mexico: Aguascalientes: Sierra Fría	LVT 10691
13	*S. a. subniger*	Mexico: Michoacán: W Zacapu	LVT 10692
16	*S. a. subniger*	Mexico: Estado de Mexico: Los Tachos	LVT 10693
19	*S. a. subniger*	Mexico: Jalisco: Nevado de Colima	LVT 10694
22	*S. s. brownorum*	Mexico: Durango: Rancho Santa Barbara	LVT 10695
25	*S. s. scalaris*	Mexico: Michoacán: Zacapu	LVT 10696
54	*S. slevini*	USA: Arizona: Chiricahua Mountains	LVT 10697
56	*S. slevini*	Mexico: Chihuahua: Sierra del Nido	LVT 10698
57	*S. chaneyi*	Mexico: Tamaulipas: Aseraderro	LVT 10699
58	*S. samcolemani*	Mexico: Nuevo León: Pablillo	LVT 10700
59	*S. samcolemani*	Mexico: Coahuila: E San Antonio de las Alazanas	LVT 10701
61	*S. bicanthalis*	Mexico: Veracruz: Xometla	AMCC 118391
179	*S. samcolemani*	Mexico: Coahuila: junction Hwy 57 and road to San Antonio de las Alazanas	LVT 10702
180	*S. samcolemani*	Mexico: Coahuila: Sierra Concordia	LVT 10703

Table 3.2. Collection and voucher data continued.

Sample ID (MX)	Taxon	Locality	Voucher Number
181	*S. s. scalaris*	Mexico: Michoacán: San Jose de Gracía	LVT 10704
182	*S. s. unicanthalis*	Mexico: Jalisco: La Primavera, Guadalajara	LVT 10705
183	*S. a. aeneus*	Mexico: Morelos: Zempoala	LVT 10706
184	*S. a. subniger*	Mexico: Querétaro: Nuevo San Joaquin	LVT 10707
185	*S. bicanthalis*	Mexico: Oaxaca: Llano de las Flores	LVT 10708
186	*S. bicanthalis*	Mexico: Oaxaca: Corral del Piedra	LVT 10709
187	*S. bicanthalis*	Mexico: Puebla: Carretera Vicente Guerrero-Alcomulga, Sierra Negra	LVT 10710
188	*S. slevini*	Mexico: Sonora: Yécora	LVT 10711
189	*S. slevini*	Mexico: Chihuahua: Mesa de Agostadero	LVT 10712
190	*S. slevini*	Mexico: Durango: Mesa de las Navar	LVT 10713
191	*S. s. scalaris*	Mexico: Querétaro: Rancho Nuevo, Pinal de Amoles	LVT 10714
193	*S. bicanthalis*	Mexico: Oaxaca: Cumbre Cerro del Cheve, Mpo. Santa Maria Papalo	LVT 10715
194	*S. s. brownorum*	Mexico: Aguascalientes: Sierra del Laurel	LVT 10716
264	*S. slevini*	USA: Arizona: Santa Rita Mountains	LVT 10717
265	*S. slevini*	USA: Arizona: Sonoita	LVT 10718
266	*S. slevini*	Mexico: Chihuahua: Creel	LVT 10719
267	*S. slevini*	Mexico: Chihuahua: Mojarachic	LVT 10720
268	*S. a. subniger*	Mexico: Estado de Mexico: Valle de Bravo	LVT 10721
269	*S. a. subniger*	Mexico: Michoacán: SE Aporo	LVT 10722

Table 3.2. Collection and voucher data continued.

Sample ID (MX)	Taxon	Locality	Voucher Number
270	*S. a. subniger*	Mexico: Michoacán: Los Azufres	LVT 10723
271	*S. a. subniger*	Mexico: Michoacán: Parque Laguna Larga	LVT 10724
272	*S. a. subniger*	Mexico: Michoacán: Mil Cumbres	LVT 10725
273	*S. s. scalaris*	Mexico: Jalisco: Tapalpa	LVT 10726
274	*S. a. subniger*	Mexico: Michoacán: N Uruapan	LVT 10727
275	*S. a. subniger*	Mexico: Michoacán: San Gregario	LVT 10728
276	*S. a. subniger*	Mexico: Hidalgo: Palo Gacho	LVT 10729
277	*S. a. subniger*	Mexico: Hidalgo: Autodromo del Angel	LVT 10730
278	*S. a. subniger*	Mexico: Querétaro: El Derramadero, Mpo. Toliman	LVT 10731
279	*S. a. subniger*	Mexico: Querétaro: Rancho Los Velázquez, Pinal de Amoles	LVT 10732
280	*S. a. subniger*	Mexico: Estado de Mexico: Villa de Carbon	LVT 10733
281	*S. s. brownorum*	Mexico: Aguascalientes: Sierra del Laurel	LVT 10734
282	*S. s. scalaris*	Mexico: San Luis Potosí: Alvarez	LVT 10735
283	*S. bicanthalis*	Mexico: Hidalgo: Tianguistengo	LVT 10736
284	*S. bicanthalis*	Mexico: Hidalgo: Calicanto	LVT 10737
285	*S. bicanthalis*	Mexico: Veracruz: Las Vigas	LVT 10738
286	*S. bicanthalis*	Mexico: Puebla: Volcán Iztaccihuatl	LVT 10739
287	*S. samcolemani*	Mexico: Nuevo León: Cerro Potosí	MVZ 144153
288	*S. samcolemani*	Mexico: Coahuila: El Taray	LVT 10740

Table 3.2. Collection and voucher data continued.

Sample ID (MX)	Taxon	Locality	Voucher Number
289	*S. samcolemani*	Mexico: Coahuila: Sierra Concordia	LVT 10741
295	*S. s. brownorum*	Mexico: Durango: Rancho Santa Barbara	LVT 10742
296	*S. slevini*	Mexico: Durango: Mesa de las Navar	LVT 10743
297	*S. s. scalaris*	Mexico: Jalisco: Tapalpa	LVT 10744
333	*S. s. unicanthalis*	Mexico: Jalisco: Sierra Manantlán	LVT 10745
334	*S. s. scalaris*	Mexico: Zacatecas: east side of state	LVT 10746
352	*S. s. scalaris*	Mexico: Puebla: Flor de Bosque	LVT 10747
392	*S. bicanthalis*	Mexico: Veracruz: Potrero Nuevo, Pico de Orizaba	LVT 10748
393	*S. bicanthalis*	Mexico: Estado de Mexico: Nevado de Toluca	LVT 10749
422	*S. s. scalaris*	Mexico: Querétaro: Rancho Nuevo, Pinal de Amoles	LVT 10750
423	*S. a. subniger*	Mexico: Puebla: Carretera "Pue 108" Jicolapa y Xochicuautla	LVT 10751
441	*S. a. subniger*	Mexico: Edo de Mexico: Chalma	LVT 10752
442	*S. a. subniger*	Mexico: Edo de Mexico: Valle de Bravo	LVT 10753
443	*S. s. brownorum*	Mexico: Aguascalientes: Sierra Fría	LVT 10754
453	*S. s. brownorum*	Mexico: Durango: Coyotes	LVT 10755
454	*S. s. brownorum*	Mexico: Durango: Otinapa	LVT 10756
455	*S. s. scalaris*	Mexico: Guanajuato: Sierra Cualtraba	LVT 10757
464	*S. slevini*	USA: New Mexico: Cloverdale	LVT 10758

Table 3.2. Collection and voucher data continued.

Sample ID (MX)	Taxon	Locality	Voucher Number
---	*S. chaneyi*	Mexico: Nuevo León: 18 km NE San Antonio Peña Nevada	GenBank U88291 (MZFC 05473)
---	*S. a. subniger*	Mexico: Tlaxcala: junction Hwy 136 with rd to Españita	GenBank U88276 (MZFC 05686)
---	*S. a. aeneus*	Mexico: Distrito Federal: El Ajusco Hwy	GenBank U88274 (BYU 45309)

Table 3.3. Outgroup samples used in this study.

Taxon	Voucher Number
Sceloporus parvus	LVT 10843
Sceloporus merriami	LSUMNS 643
Sceloporus gadoviae	T. Reeder
Sceloporus magister	T. Reeder
Sceloporus graciosus	LSUMNS 19040
Sceloporus formosus	T. Reeder
Sceloporus pointsettii	T. Reeder
Sceloporus jarrovii (*jarrovii* group)	T. Reeder
Sceloporus torquatus (*jarrovii* group)	T. Reeder
Sceloporus insignis (*jarrovii* group)	T. Reeder
Sceloporus woodi (*undulatus* group)	T. Reeder
Sceloporus cautus (*undulatus* group)	T. Reeder
Sceloporus undulatus (*undulatus* group)	T. Reeder
Phrynosoma orbiculare	LVT 10764
Holbrookia maculata	GenBank AY141063 (ND4+tRNAs), DQ001849 (ATPase 8, 6)

Table 3.4. Results of diversification rate analyses. Rate-constant and rate-variable models of diversification fit to two sets of divergence dates estimated for the *Sceloporus scalaris* group. AIC scores from the rate-constant and rate-variable models providing the best fit are noted with bold text. Alternative rate-variable models within one likelihood unit of the best-fit rate-variable model are marked with an asterisk.

	Rate-constant models		Rate-variable models			
	Pure birth	Birth–death	DDX	DDL	Yule2	Yule3
Fossil-calibrated						
lnL	-9.76	-9.76	-8.43	-4.01	-3.7	-1.5
AIC	**21.52**	23.52	20.85	**12.01**	13.4	13*
Rate-calibrated						
lnL	-14.54	-14.54	-13.29	-9.17	-7.83	-5.51
AIC	**31.08**	33.08	30.57	22.34	21.67*	**21.02**

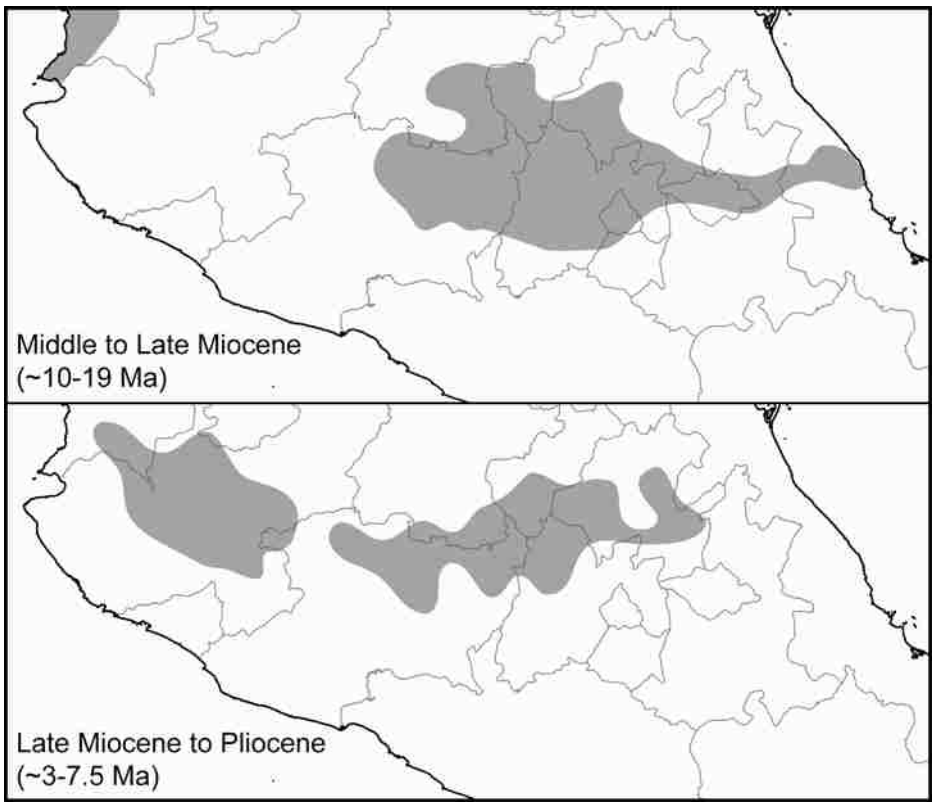

Figure 3.1. Two major volcanic episodes across the Transvolcanic Belt. These two Neogene events during the Miocene and Pliocene resulted in major mountain formations that almost completely subdivided Mexico. Extent of volcanism redrawn from Gómez-Tuena et al. (2007).

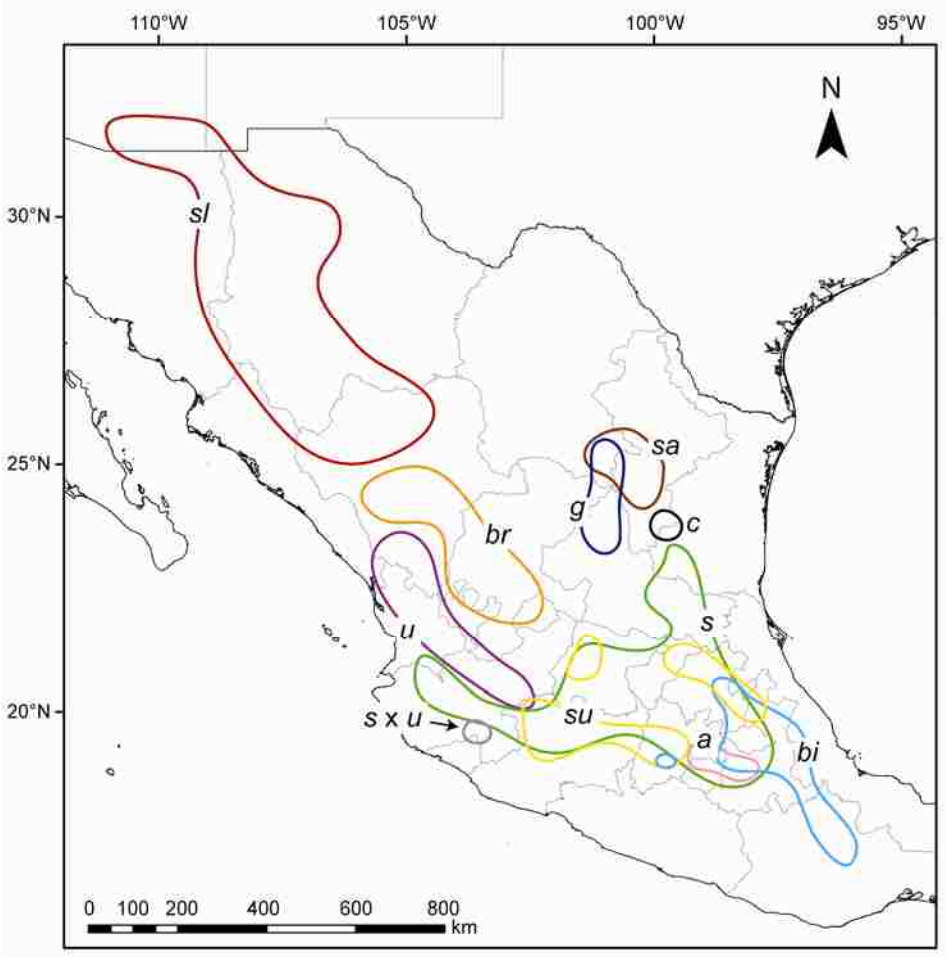

Figure 3.2. Distribution of the *Sceloporus scalaris* group. Distributions mapped following Smith et al. (1993), Smith et al. (1996), and Watkins-Colwell et al. (2005). Abbreviations are as follows: *S. slevini* (*sl*), *S. samcolemani* (*sa*), *S. chaneyi* (*c*), *S. goldmani* (*g*), *S. s. scalaris* (*s*), *S. s. brownorum* (*br*), *S. s. unicanthalis* (*u*), *S. s. scalaris* x *S. s. unicanthalis* hybrid zone (*s* x *u*), *S. a. aeneus* (*a*), *S. a. subniger* (*su*), and *S. bicanthalis* (*bi*).

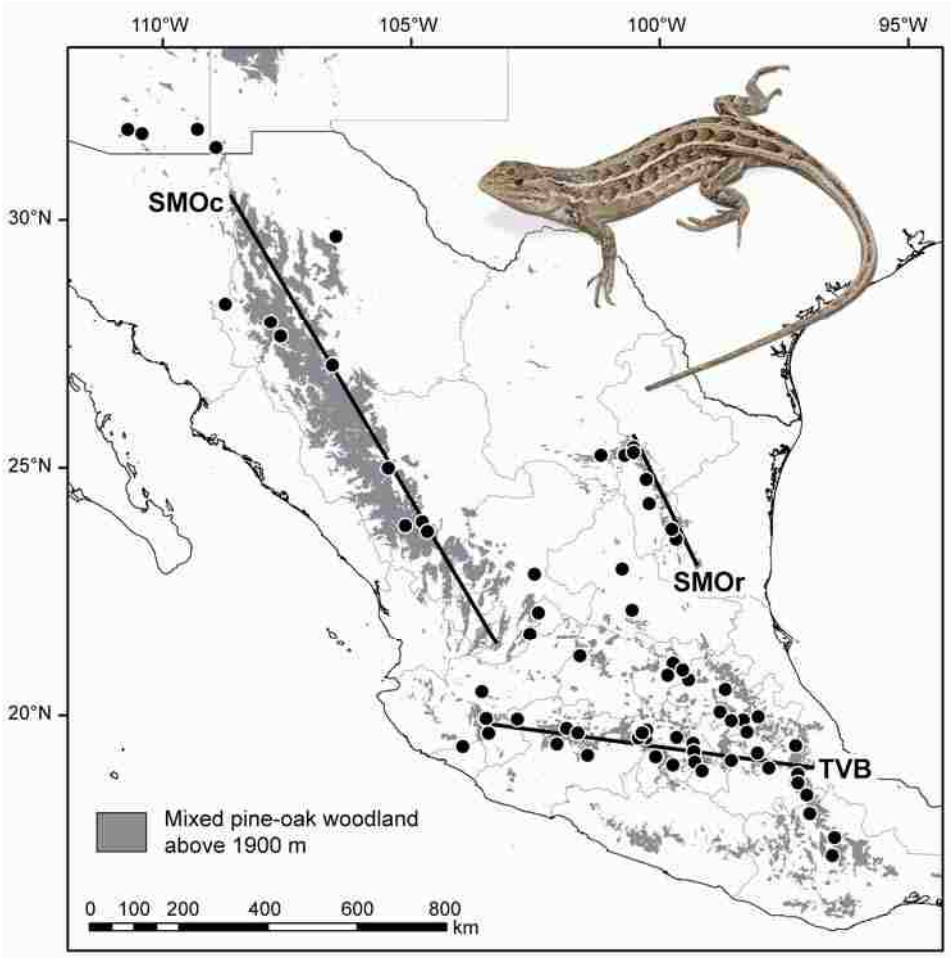

Figure 3.3. Sampling localities for genetic samples of the *Sceloporus scalaris* group overlaid on mixed pine-oak woodlands above 1900 m. Several important mountain ranges in Mexico mentioned in the text include the Transvolcanic Belt (TVB), Sierra Madre Occidental (SMOc), and northern Sierra Madre Oriental (SMOr).

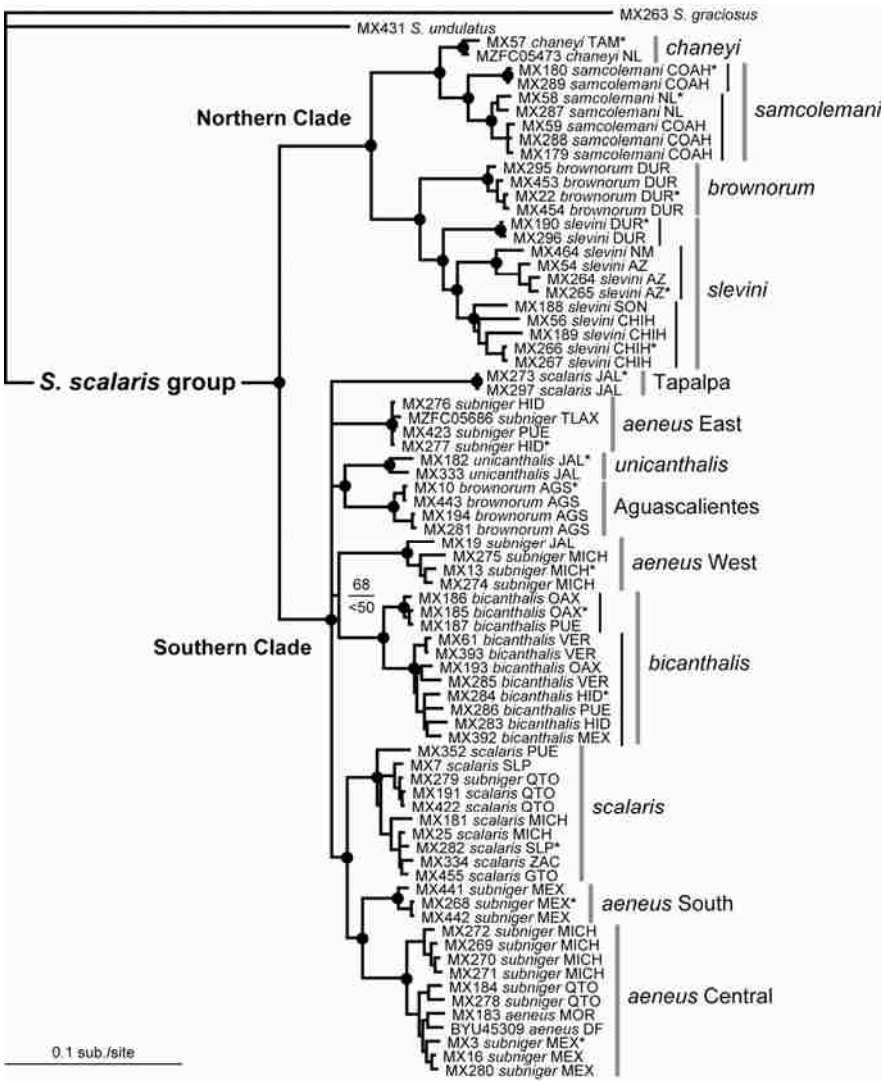

Figure 3.4. Maternal genealogy of the *Sceloporus scalaris* group based on mixed-model Bayesian inference (tree shown) and maximum likelihood analyses of mitochondrial DNA sequence data. Names of two major clades and 13 inferred lineages are indicated. Additional geographic groups nested within lineages are marked with thin black vertical lines. Numbers at nodes indicate support values (Bayesian posterior probability followed by maximum likelihood bootstrap). All major nodes that received ≥ 95% Bayesian posterior probability and ≥ 70% bootstrap support are depicted with black dots. Asterisks denote samples used in divergence dating.

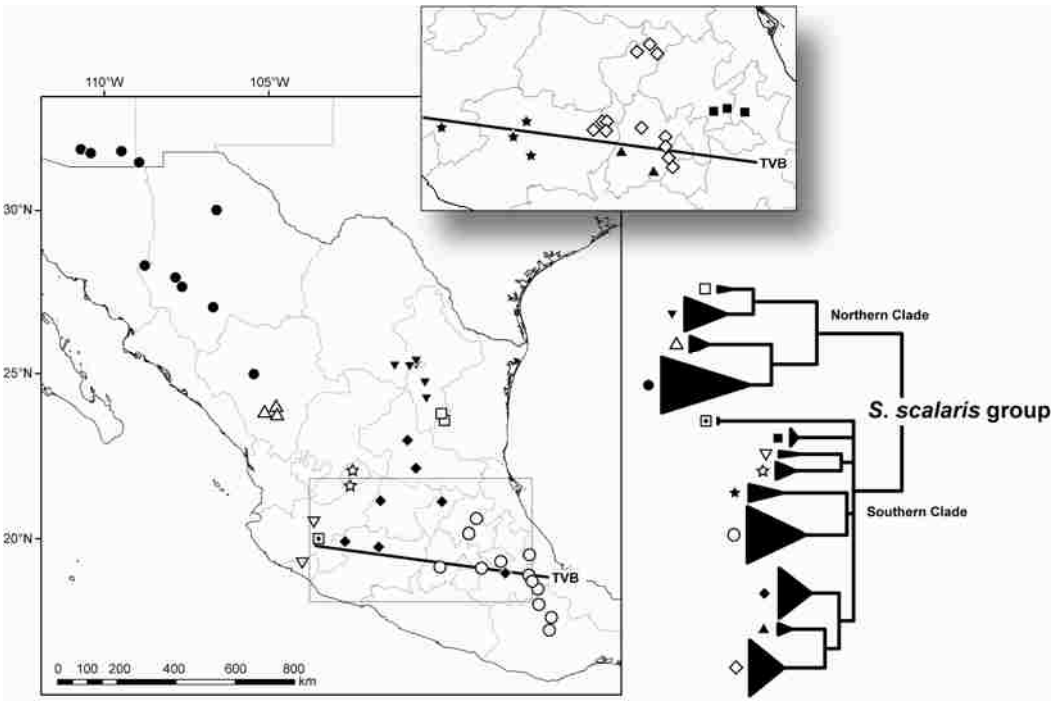

Figure 3.5. Simplified phylogeny of the *Sceloporus scalaris* group illustrating the geographic distribution of inferred haplotypes. Note approximate midpoint of the Transvolcanic Belt (TVB) in relation to lineage distributions.

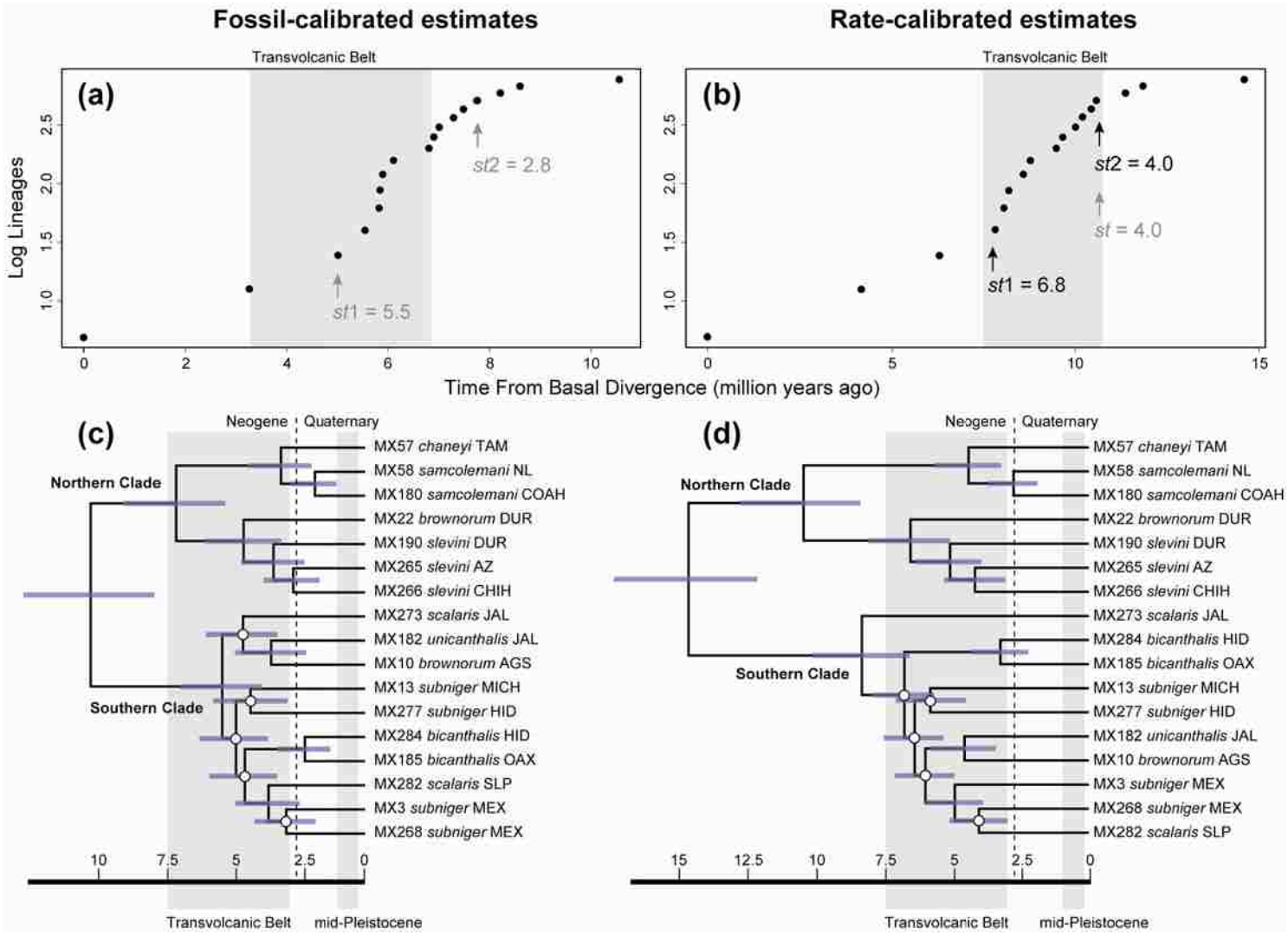
Fossil-calibrated estimates
Rate-calibrated estimates
Transvolcanic Belt
(a)
(b)
Log Lineages
st2 = 2.8
st1 = 5.5
st2 = 4.0
st = 4.0
st1 = 6.8
Time From Basal Divergence (million years ago)
(c)
(d)
Neogene
Quaternary
Northern Clade
Southern Clade
MX57 chaneyi TAM
MX58 samcolemani NL
MX180 samcolemani COAH
MX22 brownorum DUR
MX190 slevini DUR
MX265 slevini AZ
MX266 slevini CHIH
MX273 scalaris JAL
MX182 unicanthalis JAL
MX10 brownorum AGS
MX13 subniger MICH
MX277 subniger HID
MX284 bicanthalis HID
MX185 bicanthalis OAX
MX282 scalaris SLP
MX3 subniger MEX
MX268 subniger MEX
Transvolcanic Belt
mid-Pleistocene

Figure 3.6. Diversification shifts and estimated divergence dates. Lineage through time (LTT) plots derived from Bayesian relaxed clock estimates of divergence dates within the *Sceloporus scalaris* group. Dating estimates from a fossil-calibrated dataset were used to derive LTT plots in (a) and the chronogram in (c). Estimates from a rate-calibrated dataset were used to construct (b) and (d). Birth–death likelihood analyses rejected the null hypothesis of rate-constancy for both datasets. For the fossil-calibrated dataset (a), the best-fit rate-variable model was the logistic density-dependent model. An alternative rate-variable model that closely fit the dataset was the three-rate birth-death model. Estimated shifts based on this model are labeled on the plot in grey. For the rate-calibrated dataset (b), the best-fit rate-variable model was the three-rate birth-death model, with estimated rate shifts in black. An alternative rate-variable model was the two-rate birth-death model, labeled in grey. Time frames spanning a distinct volcanic episode across the Transvolcanic Belt 3–7.5 million years ago and the mid-Pleistocene pluvial-interpluvial period are depicted by grey bars. White circles denote nodes that received <90 posterior probability support. st = time of diversification rate shift.

CHAPTER 4

HISTORICAL BIOGEOGRAPHY AND DIVERSIFICATION OF THE MEXICAN ALLIGATOR LIZARD GENUS *BARISIA*

Introduction

Central to our understanding of diversification is recognition of the mechanisms that impact differentiation of species across a landscape. Many questions remain about the processes of diversification, particularly in understudied regions of high biodiversity. One such region, the Mexican highlands, is a globally important biodiversity hotspot (Mittermeier et al., 2005), yet a fundamental understanding of processes driving the origins of diversity in this region lags behind that of temperate counterparts in North America (e.g. Soltis et al., 2006; Shafer et al., 2010).

The Mexican highlands consist of four major mountain ranges spanning most of mainland Mexico (Fig. 4.1). These include the north-to-south trending Sierra Madre Occidental and Sierra Madre Oriental of northern Mexico, the east-west trending Transvolcanic Belt and Sierra Madre del Sur in central and southern Mexico, and an elevated Central Mexican Plateau. The evolutionary history of the Mexican highlands has been shaped by various geological and climatic events over the past several million years (reviewed in Bryson et al., 2011a). The relative impact of these historical events on the diversification of co-distributed montane taxa remains uncertain. Only recently have studies begun to thoroughly examine diversification in widespread Mexican montane taxa (McCormack et al., 2010; Bryson et al., 2011a; Bryson et al., in press; Bryson et al., in review). An emerging picture reveals evolutionary complexity characterized by strong geographic structuring. The relatively recent Neogene formation of the Transvolcanic

Belt in the Miocene and Pliocene appears to be a strong driver of diversification in several taxa associated with this volcanic mountain range (Bryson et al., in review). Causal mechanisms driving diversification across the remaining Mexican sierras is less clear, but may be associated with a number of filter barriers differentially subdividing lineages through time (Bryson et al., 2011a).

Alligator lizards in the genus *Barisia* are widespread across the Mexican highlands (Figs. 4.1–4.2), and inhabit mixed pine-oak woodlands from Chihuahua south to Oaxaca (Guillette and Smith, 1982; Zaldívar-Riverón and Nieto-Montes de Oca, 2002). Previous phylogenetic work (Zaldívar-Riverón et al., 2005) postulated this genus to be composed of at least five distinct species (*B. levicollis*, *B. planifrons*, *B. rudicollis*, *B. herrerae*, and *B. imbricata*) that likely diverged from one another during the Pliocene. Further, several deep lineages are embedded within the two subspecies of *B. imbricata*, *B. i. imbricata* and *B. i. ciliaris*. Investigating the tempo and mode of diversification in *Barisia* will add considerably to a fuller understanding of the complex processes structuring biological diversity in the Mexican highlands.

During the past decade, an increasingly integrative biogeography has developed tools allowing researchers to gain new insight into historical diversification processes across a landscape (see Riddle et al., 2008). Here I take advantage of a new methodological toolbox to reconstruct the evolutionary history of *Barisia*. I estimated lineage divergence dates and diversification rate from mitochondrial DNA (mtDNA) sequences, and combined divergence dates with reconstructions of ancestral geographic ranges to track lineage diversification across geography through time. Although it has been shown that single locus genetic studies have some limitations (e.g. Edwards and

Bensch, 2009), mtDNA nonetheless remains useful in exploring geographical relationships among closely-related species (e.g. Pyron and Burbrink, 2009; Daza et al., 2010; Kuriyama et al., 2011).

Methods

Taxonomic sampling and DNA sequencing

I obtained tissues from 50 *Barisia* (Table 4.1) spanning the distributions of all putative taxa within the genus (Fig. 4.2). Sequences from an additional two samples were obtained from GenBank (Table 4.1) to fill in small sampling gaps. I used *Elgaria kingii* and *Abronia graminea* as outgroups (Macey et al., 1999; Conroy et al., 2005).

I sequenced two mtDNA gene regions, including NADH dehydrogenase subunit 4 and flanking tRNAs (ND4) and a continuous region encompassing ATPase subunits 8 and 6 (ATPase 8, ATPase 6), following methods specified in Bryson et al. (2011b). These gene regions have been previously shown to be informative at different levels of divergence within lizards (Leaché and Mulcahy, 2007; Lindell et al. 2008). Primer sequences for ATPase were specifically designed for this project (C2LF4, 5'–CAATGCTCAGARATYTGYGG–3'; C3LR, 5'– GCGTGTGYTTGGTGGGTCAT–3'), and required an annealing temperature of 50 °C. Forward and reverse sequences for each individual were edited and manually aligned using Sequencher 4.2 (Gene Codes Corporation, Ann Arbor, MI).

Phylogenetic inference

Phylogenies for the mtDNA data were reconstructed using Bayesian inference (BI) and maximum likelihood (ML) methods. MrModeltest 2.1 (Nylander, 2004) was used to select a best-fit model of evolution, based on Akaike Information Criteria (AIC), for each gene region (ND4, tRNAs, ATPase 8, ATPase 6). Bayesian inference analyses were conducted on a partitioned-by-gene dataset using MrBayes 3.1 (Ronquist and Huelsenbeck, 2003). Bayesian settings included a variable rate prior, a mean branch length exponential prior of 75, and heating temperature of 0.05. All parameters except branch length and topology were unlinked between partitions. Analyses consisted of four runs (using the *nruns=4* command) for 4 x 10^6 generations using three heated and one cold Markov chain sampling every 100 generations. Output parameters were visualized using TRACER v1.4 (Rambaut and Drummond, 2007) to ascertain stationarity and convergence. All samples obtained during the first one million (25%) generations were discarded as burn-in. A 50% majority-rule consensus phylogram with nodal posterior probability support was estimated from the combination of the four runs post-burn-in. Maximum likelihood analyses were conducted using RAxML 7.0.3 (Stamatakis, 2006) with the same partitioning scheme used for the BI analyses. The GTRGAMMA model was used, and 1000 nonparametric bootstrap replicates were performed to assess nodal support. I considered those nodes with ≥ 95% Bayesian posterior probability and ≥ 70% bootstrap support as strongly supported (Hillis and Bull, 1993; Felsenstein, 2004).

Timing and tempo of diversification

Divergence dates were estimated from a partitioned-by-gene dataset of ingroup samples using BEAST v1.6.1 (Drummond and Rambaut, 2007). To calibrate my tree, I used rate calibrations for mtDNA employed previously to estimate divergences in anguid lizards (0.65–0.69% change/lineage/million years; Macey et al., 1999) and within *Barisia* (0.85% change/lineage/million years; Zaldívar-Riverón et al., 2005). I unlinked best-fit models of sequence evolution across partitions, implemented an uncorrelated lognormal clock with a Yule tree prior, and gave the ulcd.mean parameter a uniform distribution with the lower bound set to 6.5×10^{-3} substitutions/site/million years, and the upper bound set to 8.5×10^{-3} substitutions/site/million years. Analyses consisted of two independent runs each of 4×10^{7} million generations, with samples retained every 1000 generations. A Yule tree prior does not include a model of coalescence to account for intra-specific data represented in my heterogeneous dataset with both inter- and intra-specific diversity, so I ran additional analyses on a reduced dataset with only one representative from each lineage for comparison. Results were displayed in TRACER to confirm acceptable mixing and likelihood stationarity, appropriate burn-in, and adequate effective sample sizes. After discarding the first 4 million generations (10%) as burn-in, the trees and parameter estimates from the two runs were combined using LogCombiner v1.6.1 (Drummond and Rambaut, 2007). The parameter values of the samples from the posterior distribution were summarized on the maximum clade credibility tree using TreeAnnotator v1.6.1 (Drummond and Rambaut, 2007), with the posterior probability limit set to zero and mean node heights summarized.

I analyzed temporal shifts in diversification rates using ML-based diversification-rate analysis (Rabosky, 2006a) and divergence dates estimated in BEAST. The fit of different birth–death models implementing two constant rates (pure-birth, and birth–death) and four variable rates (exponential and logistic density-dependent, and two-rate and three-rate pure-birth) was computed with LASER 2.3 (Rabosky, 2006b). Model fit was measured using AIC scores. Significance of the change in AIC scores (ΔAICrc) between the best rate-constant and best rate-variable model was determined by creating a null distribution for ΔAICrc. This was done by simulating 1000 trees using yuleSim in LASER with the same number of nodes and the same speciation rate as that estimated under the pure-birth model. I additionally generated a lineage-through-time (LTT) plot using the plotLtt function in LASER to visualize the pattern of accumulation of log-lineages over time.

Ancestral area reconstruction

Ancestral areas for *Barisia* were reconstructed using a stochastic model of geographic range evolution (dispersal-extinction-cladogenesis, DEC) implemented in LAGRANGE 2.0.1 (Ree and Smith, 2008). Although the DEC model is unable to account for phylogenetic uncertainty, it can uniquely incorporate temporal and spatial constraints on range evolution that may result in more plausible area range histories (Clark et al., 2008; Ree and Smith, 2008). The maximum clade-credibility tree from BEAST analyses was used in DEC analyses, and each taxon in the genealogy was coded as present or absent in one of eight biogeographic areas based on distribution (Fig. 4.1): northern Sierra Madre Occidental, southern Sierra Madre Occidental, northern Sierra Madre Oriental, southern Sierra Madre Oriental, Transvolcanic Belt, western Sierra Madre del

Sur, and eastern Sierra Madre del Sur. The region south of the Transvolcanic Belt in Puebla, Veracruz, and northern Oaxaca has a complex geological history, and contains geological and biotic elements of both the Sierra Madre Oriental, Transvolcanic Belt, and Sierra Madre del Sur (Marshall and Liebherr, 2000; Salinas-Moreno et al., 2004; Corona et al., 2007; Paniagua and Morrone, 2009). For my analyses I considered this region as part of the Sierra Madre Oriental based on faunal affinities (Paniagua and Morrone, 2009). Range sizes were constrained to the maximum number of biogeographic regions presently inhabited by any single lineage. I additionally constrained widespread ancestors to spatially adjacent areas (Fig. 1) to exclude unlikely ranges (e.g. northern Sierra Madre Occidental + Sierra Madre del Sur).

Results

Sequence characteristics and phylogenetic estimate

The final dataset consisted of 1714 aligned nucleotide positions. Models of sequence evolution selected for partitions in both BI and BEAST analyses were GTR + I + G (ND4, ATPase 8, ATPase 6), and GTR + I (tRNA). All sequences were deposited in GenBank.

From my phylogenetic analyses I inferred 10 strongly supported lineages within three geographical clades of *Barisia* (Figs. 4.3–4.4). Four lineages corresponded to the species *B. levicollis*, *B. planifrons*, *B. rudicollis*, and *B. herrerae*. Two subspecies of *B. imbricata*, *B. i. ciliaris* and *B. i. imbricata*, appeared to each be a composite of three

distinct lineages. My sample of *B. i. jonesi* was similar to geographically adjacent samples of *B. i. imbricata*. Composition of clades are as follows:

(1) Northern clade: One lineage, *B. levicollis*, from the northern Sierra Madre Occidental.

(2) Central clade: Comprised of four lineages. Samples from the southern Sierra Madre Occidental and one sample from southern Chihuahua formed a lineage, here termed '*B. i. ciliaris* West'. A second lineage was distributed from the northern Sierra Madre Oriental across the Central Mexican Plateau ('*B. i. ciliaris* East'). This lineage also contained one sample from the southern Sierra Madre Oriental and one sample of *B. i. imbricata* from the Transvolcanic Belt. I referred to a single divergent sample from Pinal de Amoles, Querétaro as '*B. i. ciliaris* Pinal', the third lineage. Samples from the western half of Transvolcanic Belt, including the sample of *B. i. jonesi*, formed the fourth lineage '*B. i. imbricata* West'.

(3) Southern clade: Comprised of five lineages. Samples from western Michoacán east to Distrito Federal formed a '*B. i. imbricata* Central' lineage. The second lineage, '*B. i. imbricata* East', was comprised of samples distributed from Hidalgo south through Tlaxcala, Puebla, Veracruz, and northern Oaxaca, spanning the southern Sierra Madre Oriental and eastern portion of the Transvolcanic Belt. The remaining three lineages represent *B. planifrons* from the eastern Sierra Madre del Sur, and *B. rudicollis* and *B. herrerae* from the central portion of the Transvolcanic Belt.

Relationships between lineages were generally well supported with three exceptions (Fig. 4.3). The node subtending *B. i. ciliaris* West and *B. i. imbricata* West received low support (61% posterior probability and 60% bootstrap). Weak support was also inferred for the basal divergence of *B. planifrons* from *B. rudicollis*, *B. herrerae*, *B. i. imbricata* Central, and *B. i. imbricata* East (87% posterior probability and 58% bootstrap), and the divergence of *B. rudicollis* from *B. herrerae*, *B. i. imbricata* Central, and *B. i. imbricata* East (51% posterior probability and 44% bootstrap).

Divergence times and tempo of diversification

Results from analyses on the full and reduced datasets were nearly identical. Dating estimates based on analyses of the full dataset suggested that diversification in *Barisia* probably began in the Late Miocene (Table 4.2, Fig. 4.5) with an initial split between *B. levicollis* and the remaining lineages of *Barisia*. Divergences between the nine remaining lineages appeared to have followed in the Neogene. Diversification within lineages likely began near the Pliocene–Pleistocene boundary and into the Pleistocene.

Birth–death likelihood analyses rejected the null hypothesis of rate-constancy (P=0.01). The rate-variable model that best fit the dataset was the logistic density-dependent (DDL) model. Under this model, diversification rate in *Barisia* has gradually decreased through time, with diversification rate estimated at 0.8 divergences per million years (Fig. 4.6).

Ancestral area reconstruction

The maximum number of biogeographic regions inhabited within an extant lineage was four in *B. i. ciliaris* East. Optimal ancestral areas with the highest likelihood scores and probabilities were identified at each node (Fig. 4.5). Alternative ancestral areas within 2 log-likelihood units were summarized in Table 4.2. One node with alternative ancestral areas (node 6) appeared unresolved; probabilities between alternative reconstructions differed by less than 10%. Initial diversification within *Barisia* (node 1) probably occurred between the northern Sierra Madre Occidental and a widespread common ancestor distributed across the Sierra Madre Occidental, southern Sierra Madre Oriental, and Transvolcanic Belt. This widespread ancestor was later fragmented within the Transvolcanic Belt (node 2), and the ancestor within the Transvolcanic Belt subsequently split four times across this mountain range (nodes 6–9) and dispersed into the eastern Sierra Madre del Sur. The remaining ancestor distributed across the Sierra Madre Occidental, southern Sierra Madre Oriental, and Transvolcanic Belt later diverged within the southern Sierra Madre Oriental (node 3) before splitting apart (nodes 4 and 5). Colonization of the western isolate of the Sierra Madre del Sur occurred relatively recently from the Transvolcanic Belt (node not shown).

Discussion

Based on my results, alligator lizards in the genus *Barisia* have had a long history in the Mexican highlands. Diversification likely began in the Late Miocene in a wide-ranging ancestor distributed across the Sierra Madre Occidental, Transvolcanic Belt, and

southern Sierra Madre Oriental (Fig. 4.5). Following this initial split at about 11 Ma, a second divergence occurred within this wide-ranging ancestor at around 9 Ma, and two geographical clades subsequently emerged. Divergences within these regional clades appear to have happened during distinctly different temporal periods. A southern clade distributed across the Transvolcanic Belt and into the eastern Sierra Madre del Sur split rapidly between 6–8 Ma into five lineages (*B. planifrons*, *B. herrerae*, and *B. i. imbricata* Central and East). Afterwards, diversification across a broader landscape between 3–5 Ma led to the formation of the four lineages within the northern clade (*B. i. ciliaris* Pinal, *B. i. ciliaris* East and West, and *B. i. imbricata* West).

Lineage diversification in *Barisia* during the Neogene appears linked with the development of the Transvolcanic Belt (Fig. 4.5). The formation of this mountain range across south-central Mexico impacted diversification in a range of highland and lowland taxa (Bryson et al., 2011b). Uplift of the Transvolcanic Belt created new geographical barriers and united previously isolated highland biotas. Five lineages of *Barisia* are broadly distributed across the Transvolcanic Belt (Fig. 4.4). Mean estimated divergence dates between all five of these lineages (Table 4.2) fall near or within a second major episode of widespread volcanism along the Transvolcanic Belt in the Neogene (Fig. 4.5) (Gómez-Tuena et al., 2007). Because of the relatively young geological age of this second episode, the extensive uplifting likely left a large evolutionary imprint on the genetic structures of extant lineages that has not yet eroded through time. Indeed, a variety of co-distributed taxa associated with the Transvolcanic Belt demonstrate genetic divergences temporally congruent with this second period of Transvolcanic Belt formation, including fish (Hulsey et al., 2004), amphibians (Mulcahy and Mendelson,

2000), reptiles (Bryson et al., 2011a; Bryson et al., 2011b; Bryson et al., in press; Bryson et al., in review), and birds (McCormack et al., 2008, 2010).

The diversification rate within *Barisia* appears to be slowly declining (Fig. 4.6). A period of initial widespread uplifting of the Transvolcanic Belt between about 10–19 Ma (Gómez-Tuena et al., 2007) may have created a highland corridor that promoted dispersal between the montane biotas of the Sierra Madre Occidental and Sierra Madre Oriental. This Late Miocene linkage could explain my reconstruction of initial fragmentation around 11 Ma of a widespread common ancestor distributed across the Sierra Madre Occidental, Transvolcanic Belt, and southern Sierra Madre Oriental. Similar patterns of deep divergences between largely northern and southern highland clades (Bryson et al., in review) might also be attributed to an early connection of highland biotas across the Transvolcanic Belt. A second episode of widespread uplifting across the Miocene–Pliocene boundary may have subsequently divided *Barisia* distributed along the Transvolcanic Belt. *Barisia* to the north were later likely fragmented during the Pliocene, perhaps as filter barriers such as major river drainages (Bryson et al., 2011a) formed and subdivided lineages.

Diversification within several widespread lineages of *Barisia* such as *B. i. ciliaris* West and East and *B. i. imbricata* East appear to date to near the Pliocene–Pleistocene boundary. However, an overall lack of clear geographic partitioning of genetic diversity within these and other lineages (Figs. 4.3–4.4) makes inferences on the historical processes responsible for within-lineage diversification difficult. Expansions of pine-oak woodlands during Pleistocene glacial cycles (Gugger et al., 2010; Bryson et al., in press) may have promoted dispersal and periodic bouts of gene flow that could have erased or

obscured previously acquired signals of historical isolation in *Barisia*. Future studies utilizing multilocus data within a coalescent framework should better delineate major lineages of *Barisia*.

Results from my study are broadly congruent with results from a previous study (Zaldívar-Riverón et al., 2005) with few notable exceptions. My range-wide sampling not only helped further delineate distributions of mtDNA lineages, but also elucidated the discovery of a deeply divergent lineage, *B. levicollis*. Zaldívar-Riverón et al. (2005), lacking molecular data for *B. levicollis* and relying on morphology, suggested a close relationship between this species and northern populations of *B. i. ciliaris* (Zaldívar-Riverón et al., 2005). My data suggests *B. levicollis* might instead be a paleoendemic restricted to the northern Sierra Madre Occidental, sister to all other *Barisia*. Further, based on my results, localities of two samples used previously appear to be reversed ("*B. i. imbricata*2" and "*B. i. imbricata*8"). This is additionally confirmed by my comparison of ND4 sequences from identical (Mil Cumbres, Michoacán) and nearby (Pico de Orizaba and Xometla, Veracruz) localities. Reversing OTUs in the combined phylogenetic analyses of Zaldívar-Riverón et al. (2005) might change their results on the evolution of dorsal pattern in these lizards.

As with other taxa restricted to the highlands of Mexico, *Barisia* are threatened by an ever-expanding human population and habitat destruction. At least two species (*B. rudicollis* and *B. herrerae*) are confined to a relatively small region adjacent to one of the world's most populated areas, and both species may already be in decline (Zaldívar-Riverón and Nieto-Montes de Oca, 2002). *Barisia rudicollis* and *B. herrerae* are considered endangered by the International Union for Conservation of Nature (Flores-

Villela and Canseco-Márquez, 2007). Another distinct lineage inferred in my study from near Pinal de Amoles, Querétaro may also have a small range. Future studies should focus on further delineating evolutionary distinct taxa within *Barisia*. These findings viewed in concert with previous phylogeographic studies may fuel new interest in elucidating potentially hidden yet critically threatened components of a unique Mexican highland biota.

Table 4.1. Collection and voucher data for genetic samples of *Barisia* used in this study. All samples deposited in the Las Vegas Tissue Collection (LVT), Ambrose Monell Cryo Collection (AMCC), or Museum of Vertebrate Zoology, University of California, Berkeley (MVZ).

Sample ID (MX)	Taxon	Locality	Voucher Number
2	*B. i. ciliaris*	Mexico: Nuevo León: Pablillo	LVT 10795
6	*B. i. ciliaris*	Mexico: Coahuila: Santa Rita	LVT 10796
9	*B. i. imbricata*	Mexico: Jalisco: Volcán Tequila	LVT 10797
15	*B. i. ciliaris*	Mexico: Durango: Rancho Santa Barbara	LVT 10798
21	*B. i. ciliaris*	Mexico: Tamaulipas: Aserradero	LVT 10799
24	*B. planifrons*	Mexico: Oaxaca: Sierra Monte Flor	LVT 10800
36	*B. levicollis*	Mexico: Chihuahua: Sierra del Nido	LVT 10801
55	*B. i. ciliaris*	Mexico: Aguascalientes: Sierra Fría	LVT 10802
60	*B. i. imbricata*	Mexico: Veracruz: Xometla	AMCC 118392
62	*B. i. imbricata*	Mexico: Puebla: Sierra Negra	AMCC 118355
63	*B. planifrons*	Mexico: Oaxaca: Cerro San Felipe	AMCC 117877
69	*B. i. imbricata*	Mexico: Jalisco: Volcán del Fuego	LVT 10803
72	*B. i. imbricata*	Mexico: Estado de México: Chapa de Mota	LVT 10804
195	*B. i. ciliaris*	Mexico: Guanajuato: Sierra Santa Rosa	LVT 10805
196	*B. i. imbricata*	Mexico: Michoacán: Cerro Tancítaro	LVT 10806
197	*B. i. imbricata*	Mexico: Veracruz: Las Vigas	LVT 10807
198	*B. i. imbricata*	Mexico: Puebla: Volcán Iztaccihuatl	LVT 10808
199	*B. i. ciliaris*	Mexico: Querétaro: Nuevo San Joaquin	LVT 10809

Table 4.1. Collection and voucher data continued.

Sample ID (MX)	Taxon	Locality	Voucher Number
200	*B. i. imbricata*	Mexico: Estado de México: Atlacomulco	LVT 10810
201	*B. i. imbricata*	Mexico: Michoacán: Parque José María Morelos	LVT 10811
202	*B. levicollis*	Mexico: Chihuahua: Sierra del Nido	LVT 10812
203	*B. i. ciliaris*	Mexico: Chihuahua: Mesa de Agostadero	LVT 10813
302	*B. i. imbricata*	Mexico: Michoacán: Tacambaro	LVT 10814
303	*B. i. imbricata*	Mexico: Michoacán: Mil Cumbres	LVT 10815
304	*B. i. imbricata*	Mexico: Michoacán: SE Aporo	LVT 10816
305	*B. i. imbricata*	Mexico: Hidalgo: Calicanto	LVT 10817
306	*B. i. jonesi*	Mexico: Michoacán: Dos Aguas	LVT 10818
307	*B. i. imbricata*	Mexico: Tlaxcala: Apizaco	LVT 10819
308	*B. i. imbricata*	Mexico: Morelos: Zempoala	LVT 10820
309	*B. i. ciliaris*	Mexico: Querétaro: Cerro Zamorano	LVT 10821
310	*B. rudicollis*	Mexico: Estado de México: Valle de Bravo	LVT 10822
311	*B. herrerae*	Mexico: Estado de México: Ocuilan	LVT 10823
312	*B. i. imbricata*	Mexico: Jalisco: Tapalpa	LVT 10824
313	*B. i. ciliaris*	Mexico: Durango: Mesa de las Navar	LVT 10825
314	*B. i. ciliaris*	Mexico: San Luis Potosí: Alvarez	LVT 10826
315	*B. i. ciliaris*	Mexico: Querétaro: Rancho Los Velázquez, Pinal de Amoles	LVT 10827
316	*B. i. imbricata*	Mexico: Estado de México: Llano Grande	LVT 10828
317	*B. i. imbricata*	Mexico: Distrito Federal: Sierra Ajusco	LVT 10829

Table 4.1. Collection and voucher data continued.

Sample ID (MX)	Taxon	Locality	Voucher Number
318	*B. planifrons*	Mexico: Oaxaca: Ixtlán de Juárez	LVT 10830
319	*B. planifrons*	Mexico: Oaxaca: Yuvila	LVT 10831
320	*B. i. imbricata*	Mexico: Oaxaca: Peña Verde	LVT 10832
321	*B. i. imbricata*	Mexico: Estado de México: Rio Frio	MVZ 191048
322	*B. i. imbricata*	Mexico: Hidalgo: Eloxochitlán	LVT 10833
338	*B. levicollis*	Mexico: Chihuahua: Creel	LVT 10834
339	*B. levicollis*	Mexico: Chihuahua: Ejido Zorillo	LVT 10835
402	*B. i. imbricata*	Mexico: Michoacán: Cerro Angahuan	LVT 10836
437	*B. i. imbricata*	Mexico: Guerrero: Sierra Taxco	LVT 10837
438	*B. i. ciliaris*	Mexico: San Luis Potosí: Real de Catorce	LVT 10838
439	*B. i. ciliaris*	Mexico: Jalisco: Sierra Huichol	LVT 10839
440	*B. herrerae*	Mexico: Estado de México: Ocuilan	LVT 10840
--	*B. i. imbricata*	Mexico: Jalisco: Manantlán	GenBank AY605116
--	*B. rudicollis*	Mexico: Michoacán: El Pinal, Mpo. Tuxpan	GenBank AY605121
--	*Elgaria kingii*	Mexico: Chihuahua: Sierra del Nido	LVT 10841
--	*Abronia graminea*	Mexico: Veracruz: Puerto del Aire	LVT 10842

Table 4.2. Estimated divergence dates within *Barisia* derived from Bayesian relaxed clock estimates. Numbers refer to nodes identified in Figure 5. Posterior mean ages and 95% highest posterior density intervals (HPD) provided in millions of years ago. Ancestral areas reconstructed for each node are followed by relative probability values. Area reconstructions at each node are the split of areas inherited by the two descendent branches (upper branch followed by lower branch). The optimal ancestral areas with the highest probabilities were selected among the alternatives and presented in Fig. 5. Abbreviations as follows: Sierra Madre Occidental (SMOc), Sierra Madre Oriental (SMOr), Central Mexican Plateau (CMP), Transvolcanic Belt (TVB), and Sierra Madre del Sur (SMS).

Node	Posterior mean age (95% HPD)	Ancestral area (rel. prob.)
1	11 (8.4–13.7)	northern SMOc / northern SMOc + southern SMOc + southern SMOr + TVB (0.33)
2	8.9 (7.2–10.7)	northern SMOc + southern SMOc + southern SMOr + TVB / TVB (0.39)
3	5.1 (3.9–6.3)	southern SMOr / northern SMOc + southern SMOc + southern SMOr + TVB (0.34)
		southern SMOr / northern SMOc + southern SMOc + CMP + TVB (0.21)
		southern SMOr / northern SMOc + southern SMOc + TVB (0.15)
4	3.7 (2.9–4.5)	southern SMOr / northern SMOc + southern SMOc + TVB (0.36)
		northern SMOr + southern SMOr + CMP + TVB / TVB (0.26)
		TVB / northern SMOc + southern SMOc + TVB (0.12)
5	3.4 (2.7–4.1)	northern SMOc + southern SMOc / TVB (0.56)
		southern SMOc / TVB (0.36)

Table 4.2. Estimated divergence dates and ancestral area reconstructions continued.

Node	Posterior mean age (95% HPD)	Ancestral area (rel. prob.)
6	8 (6.4–9.7)	TVB / TVB (0.50)
		eastern SMS / TVB (0.47)
7	7.7 (6.2–9.4)	TVB / TVB (0.99)
8	6.7 (5.4–8.2)	TVB / TVB (0.97)
9	6.1 (4.8–7.4)	TVB / TVB (0.88)

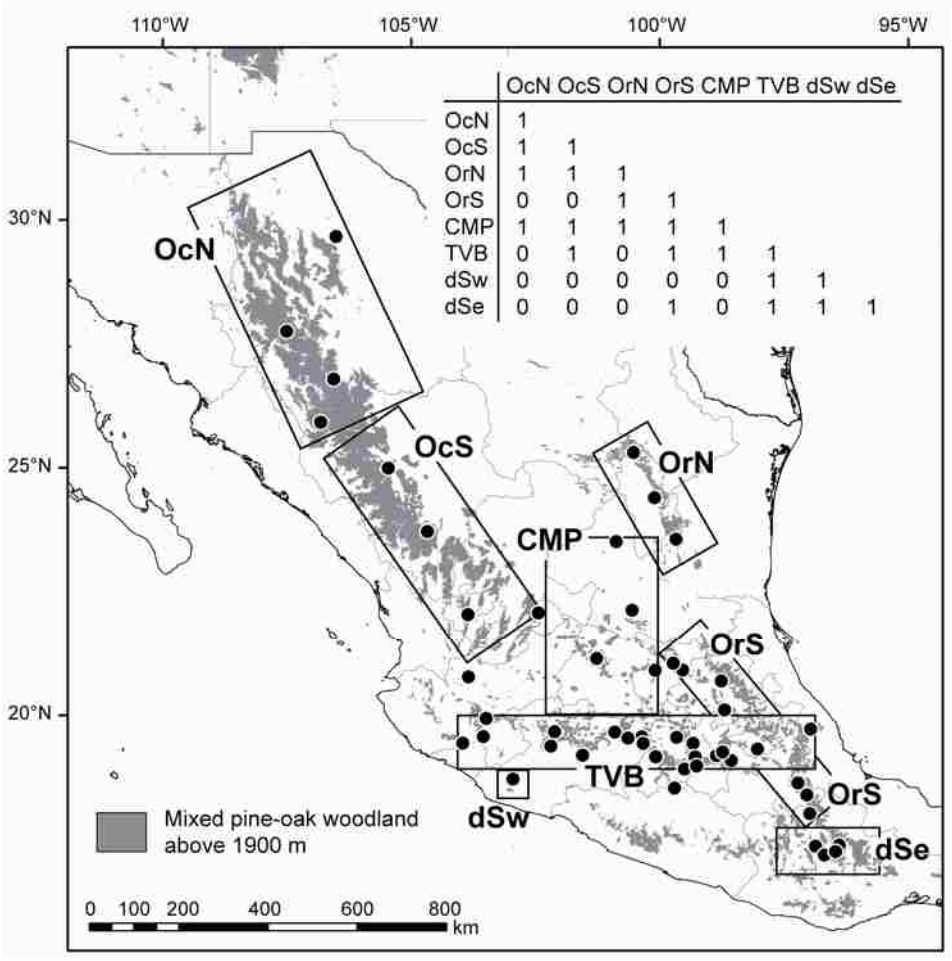

Figure 4.1. Map depicting the highlands of Mexico. Localities of genetic samples used in study are overlaid on mixed pine-oak forests above 1900 meters. Biogeographic areas include the northern Sierra Madre Occidental (OcN), southern Sierra Madre Occidental (OcS), northern Sierra Madre Oriental (OrN), southern Sierra Madre Oriental (OrS), Central Mexican Plateau (CMP), Transvolcanic Belt (TVB), eastern Sierra Madre del Sur (dSe), and western Sierra Madre del Sur (dSw). For ancestral area reconstructions, an area adjacency matrix was used (upper right corner) to restrict ranges to geographically proximate areas.

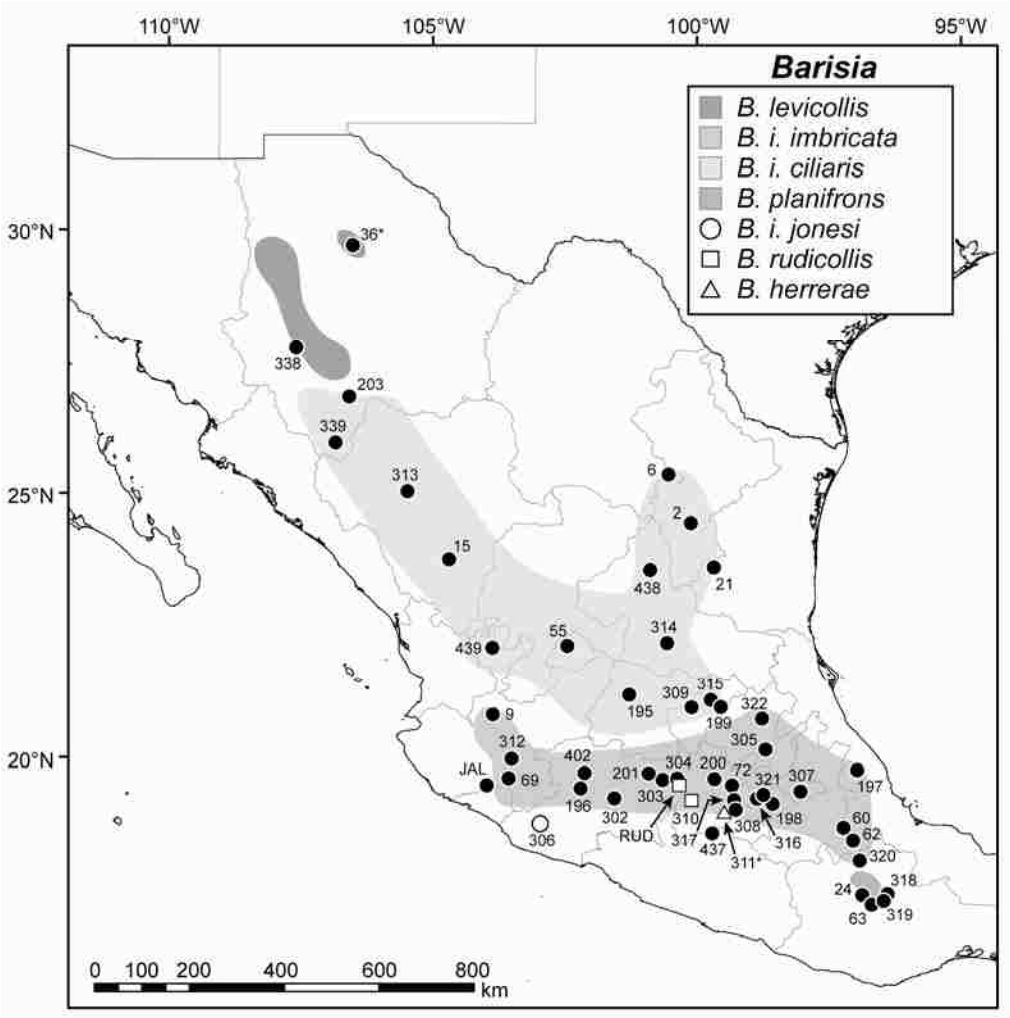

Figure 4.2. Localities of genetic samples used and distribution (adapted from Zaldívar-Riverón et al., 2005) of taxa in the genus *Barisia*. Asterisks denote multiple samples used from the same locality. The prefix 'MX' was omitted from sample numbers for clarity.

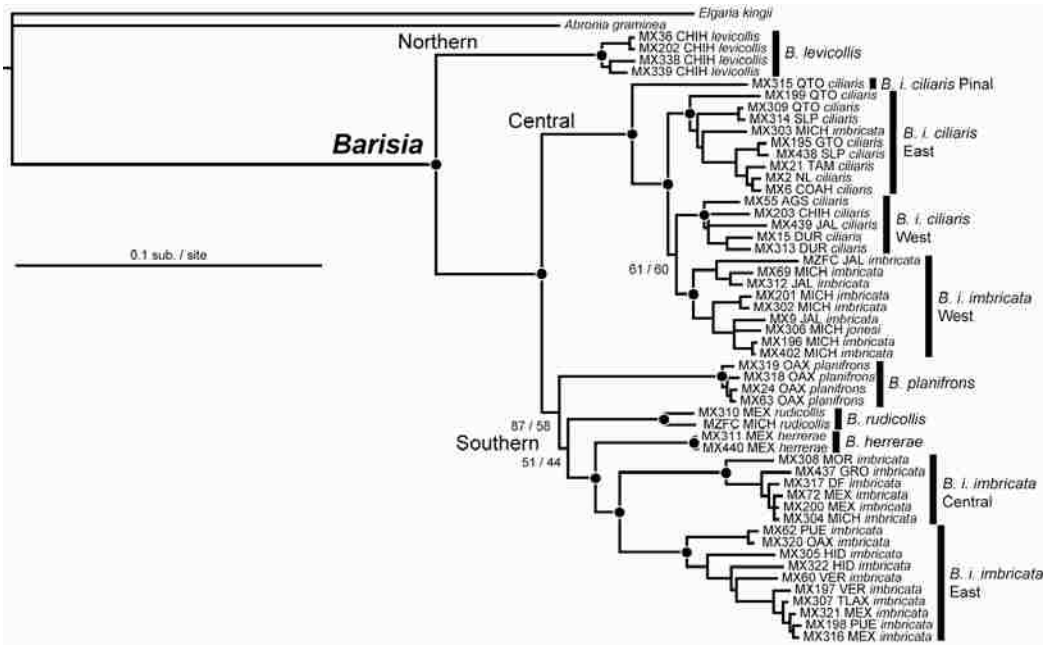

Figure 4.3. Maternal genealogy of *Barisia* based on mixed-model Bayesian inference (tree shown) and maximum likelihood analyses of mitochondrial DNA sequence data. Numbers at nodes indicate support values (Bayesian posterior probability followed by maximum likelihood bootstrap). Nodes that received ≥ 95% Bayesian posterior probability and ≥ 70% bootstrap support are depicted with black dots.

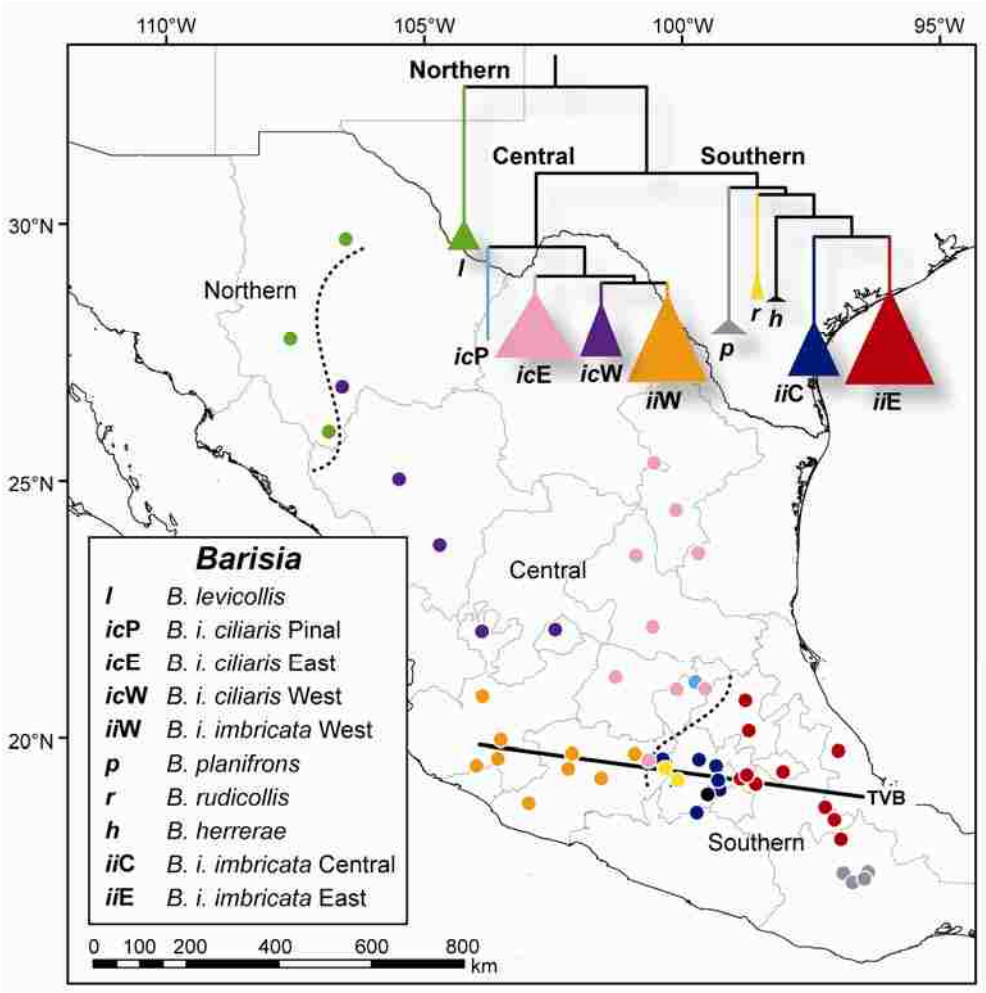

Figure 4.4. Geographical distribution of inferred mitochondrial lineages within *Barisia*. Lineages are color-coded to correspond to haplotypes plotted on map. Dotted lines denote approximate breaks between northern, central, and southern clades. Note midpoint of the Transvolcanic Belt (TVB) in relation to lineage distributions.

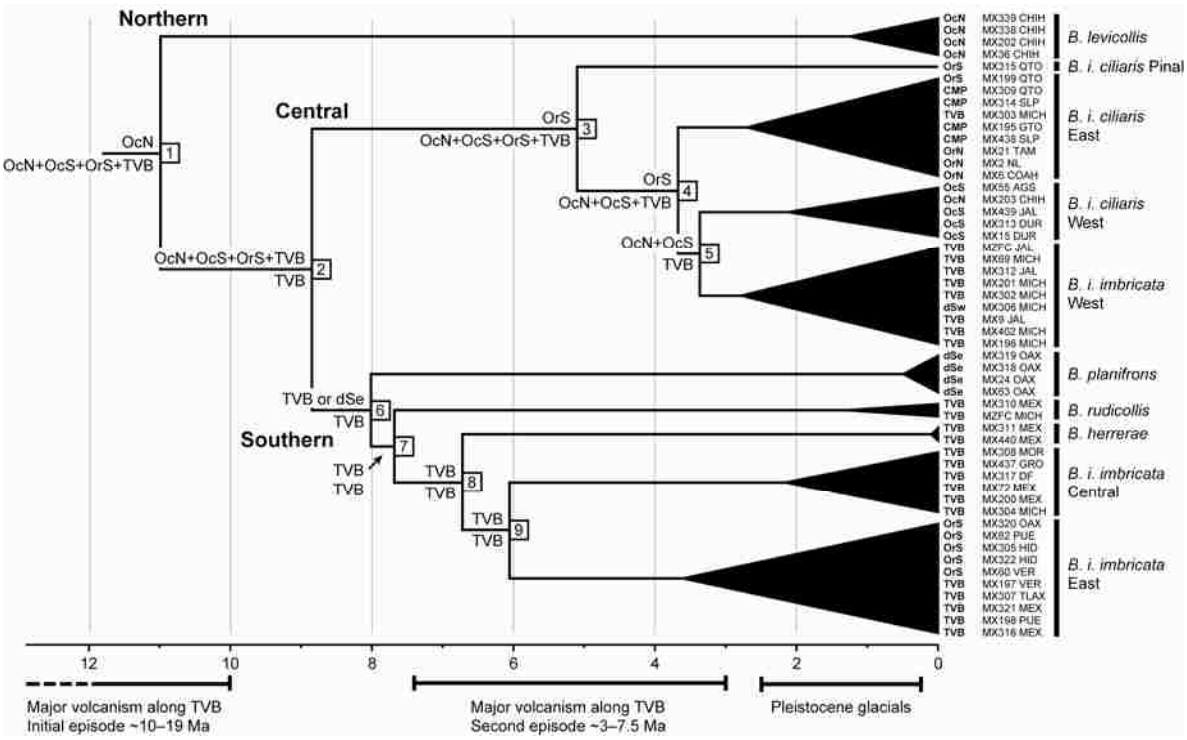

Figure 4.5. Chronogram for lineage divergences within *Barisia* and maximum likelihood reconstruction of geographic range evolution. Optimal ancestral areas with the highest likelihood scores and the highest probabilities are presented at each node. Alternative ancestral areas within 2 log-likelihood units and estimated divergence dates for numbered nodes can be found in Table 4.2. Time frames spanning two distinct volcanic episodes across the Transvolcanic Belt and the Pleistocene period are shown. Biogeographic areas are delineated in Fig. 4.1 and are as follows: northern Sierra Madre Occidental (OcN), southern Sierra Madre Occidental (OcS), northern Sierra Madre Oriental (OrN), southern Sierra Madre Oriental (OrS), Central Mexican Plateau (CMP), Transvolcanic Belt (TVB), eastern Sierra Madre del Sur (dSe), and western Sierra Madre del Sur (dSw).

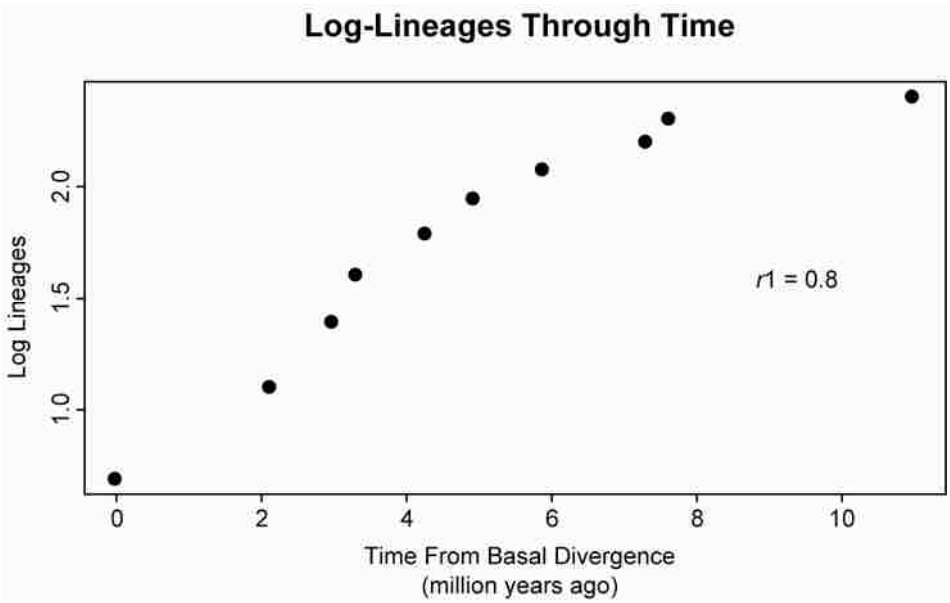

Figure 4.6. Lineage through time plot derived from Bayesian relaxed clock estimates of divergence dates within *Barisia*. Birth–death likelihood analyses suggest a gradual decrease in diversification rate though time, with diversification rate (r) estimated at 0.8 divergences per million years.

BIBLIOGRAPHY

Anducho-Reyes, M.A., Cognato, A.I., Hayes, J.L., Zuniga, G., 2008. Phylogeography of the bark beetle *Dendroctonus mexicanus* Hopkins (Coleoptera: Curculionidae: Scolytinae). Mol. Phylgenet. Evol. 49, 930–940.

Arévalo, E., Davis, S.K., Sites, Jr. J., 1994. Mitochondrial DNA sequence divergence and phylogenetic relationships among eight chromosome races of the *Sceloporus grammicus* complex (Phrynosomatidae) in Central Mexico. Syst. Biol. 43, 387–418.

Barrowclough, G.F., Zink, R.M., 2009. Funds enough, and time: mtDNA, nuDNA and the discovery of divergence. Mol. Ecol. 18, 2934–2936.

Benabib, M., Kjer, K.M., Sites, Jr. J.W., 1997. Mitochondrial DNA sequence-based phylogeny and the evolution of viviparity in the Sceloporus scalaris group (Reptilia, Squamata). Evolution 51, 1262-75.

Brower, L.P., Castilleja, G., Peralta, A., Lopez-Garcia, J., Bojorquez-Tapia, L., Diaz, S., Melgarejo, D., Missrie, M., 2002. Quantitative changes in forest quality in a principal overwintering area of the monarch butterfly in Mexico, 1971–1999. Conserv. Biol. 16, 346–359.

Bryson, R.W., Pastorini, J., Burbrink, F.T., Forstner, M.R.J., 2007. A phylogeny of the *Lampropeltis mexicana* complex (Serpentes: Colubridae) based on mitochondrial DNA sequences suggests evidence for species-level polyphyly within *Lampropeltis*. Mol. Phylogenet. Evol. 43, 674–684.

Bryson, R.W., Nieto-Montes de Oca, A., Jaeger, J.R., Riddle, B.R., 2010. Elucidation of cryptic diversity in a widespread Nearctic treefrog reveals episodes of mitochondrial gene capture as frogs diversified across a dynamic landscape. Evolution 64, 2315-2330.

Bryson, R.W., Murphy, R.W., Lathrop, A., Lazcano-Villareal, D., 2011a. Evolutionary drivers of phylogeographical diversity in the highlands of Mexico: a case study of the *Crotalus triseriatus* species group of montane rattlesnakes. J. Biogeogr. 38, 697–710.

Bryson, R.W., García-Vázquez, U.O., Riddle, B.R., 2011b. Phylogeography of Middle American gophersnakes: Mixed responses to biogeographical barriers across the Mexican Transition Zone. J. Biogeogr. DOI: 10.1111/j.1365-2699.2011.02508.x

Bryson, R.W., Murphy, R.W., Graham, M.R., Lathrop, A., Lazcano-Villareal, D., In press. Historical diversification of the *Crotalus intermedius* group and Pleistocene pine-oak woodland connections between Mexico's Sierra Madre Occidental and Sierra Madre Oriental. J. Biogeogr.

Bryson, R.W., García-Vázquez, U.O., Riddle, B.R., In review. Testing the roles of Neogene vicariance and Quaternary climate change on the historical diversification of bunchgrass lizards (*Sceloporus scalaris* group) in Mexico. Mol. Phylogen. Evol.

Burney, C.W., Brumfield, R.T., 2009. Ecology predicts levels of genetic differentiation in Neotropical birds. Am. Nat. 174, 358–368.

Campbell, J.A., Lamar, W.W., 2004. Venomous Reptiles of the Western Hemisphere. Cornell University Press, Ithaca, New York.

Carreño, A.L., Helenes, J., 2002. Geology and ages of the islands. In: Case, T.J., Cody, M.L., Ezcurra, E. (Eds.) A New Island Biogeography of the Sea of Cortés. Oxford University Press, New York, pp. 14–40.

Castoe, T.A., Spencer, C.L., Parkinson, C.L., 2007. Phylogeographic structure and historical demography of the western diamondback rattlesnake (*Crotalus atrox*): a perspective on North American desert biogeography. Mol. Phylogenet. Evol. 42, 193–212.

Castoe, T.A., Daza, J.M., Smith, E.N., Sasa, M.M., Kuch, U., Campbell, J.A., Chippindale, P.T., Parkinson, C.L., 2009. Comparative phylogeography of pitvipers suggests a consensus of ancient Middle American highland biogeography. J. Biogeogr. 36, 88–103.

Challenger, A., 1998. Utilización y Conservación de los Ecosistemas Terrestres de México. Pasado, Presenté y Yuturo. CONABIO, México, D.F.

Chan, K.M.A., Moore, B.R., 2005. SymmeTREE: Whole-tree analysis of differential diversification rates. Bioinformatics 21, 1709–1710.

Clark, J.R., Ree, R.H., Alfaro, M.E., King, M.G., Wagner, W.L., Roalson, E.H., 2008. A comparative study in ancestral range reconstruction methods: retracing the uncertain histories of insular lineages. Sys. Biol. 57, 693–707.

Conroy, C.J., Bryson, R.W., Lazcano, D., Knight, A., 2005. Phylogenetic position of the pygmy alligator lizard based on mitochondrial DNA. J. Herpetol. 39, 142–147.

Corona, A.M., Toledo, V.H., Morrone, J.J., 2007. Does the Trans-Mexican Volcanic Belt represent a natural biogeographic unit? An analysis of the distributional patterns of Coleoptera. J. Biogeogr. 34, 1008–1015.

Daza, J.M., Castoe, T.A., Parkinson, C.L., 2010. Using regional comparative phylogeographic data from snake lineages to infer historical processess in Middle America. Ecography 33, 343–354.

Devitt, T.J., 2006. Phylogeography of the Western Lyresnake (*Trimorphodon biscutatus*): testing aridland biogeographical hypotheses across the Nearctic–Neotropical transition. Mol. Ecol. 15, 4387–4407.

Dixon, J.R., Lemos-Espinal, J.A., 2010. Anfibios y Reptiles del Estado de Querétaro, México. Amphibians and Reptiles of the State of Querétaro, México. México. CONABIO, México, D.F.

Drummond, A.J., Rambaut, A., 2007. BEAST: Bayesian evolutionary analysis by sampling trees. BMC Evol. Biol. 7, 214.

Edwards, S., Bensch, S., 2009. Looking forwards or looking backwards in avian phylogeography? A comment on Zink and Barrowclough 2008. Mol. Ecol. 18, 2930–2933.

Estes, R., 1983. Sauria terrestria, Amphisbaenia. In: Handbuch der Paläoherpetologie, pp. 1–249. Edited by: Wellnhofer, P. Stuttgart, NY: Gustav Fischer Verlag.

Farjon, A., Styles, B.T., 1997. Flora Neotropica: *Pinus* (Pinaceae). New York Botanical Garden, New York, NY.

Felsenstein, J., 2004. Inferring Phylogenies. Sinauer Associates, Sunderland, MA.

Ferrusquía-Villafranca, I., 1993. Geology of Mexico: a synopsis. In: Biological Diversity of Mexico: Origins and Distribution, pp. 3–107. Edited by: Ramamoorthy, T.P., Bye, R.A., Lot, A., Fa, J. Oxford, NY: Oxford University Press.

Ferrusquía-Villafranca, I., González-Guzmán, L.I., 2005. Northern Mexico's landscape, part II: the biotic setting across time. In: Biodiversity, Ecosystems, and Conservation in Northern Mexico, pp. 39–51. Edited by: Cartron, J.-L.E., Ceballos, G., Felger, R.S. Oxford, NY: Oxford University Press.

Flores-Villela, O., Canseco-Márquez, L., 2007. *Barisia herrerae*. In: IUCN 2010. IUCN Red List of Threatened Species. Version 2010.4. <www.iucnredlist.org>. Downloaded on 04 April 2011.

Flores-Villela, O., Martínez-Salazar, E.A., 2009. Historical explanation of the origin of the herpetofauna of Mexico. Rev. Mex. Biodivers. 80, 817–833.

Galicia, L., García-Romero, A., 2007. Land use and land cover change in highland temperate forests in the Izta-Popo National Park, Central Mexico. Mountain Res. Development 27, 48–57.

Godinho, R., Crespo, E.G., Ferrand, N., 2008. The limits of mtDNA phylogeography: complex patterns of population history in a highly structured Iberian lizard are only revealed by the use of nuclear markers. Mol. Ecol. 17, 4670-4683.

Gómez-Tuena, A., Orozco-Esquivel, Ma.T., Ferrari, L., 2007. Igneous petrogenesis of the Trans-Mexican Volcanic Belt. Geol. Soc. Am. Special Paper 422, 129–181.

Gugger, P.F., Gonzalez-Rodriguez, A., Rodriguez-Correa, H., Sugita, S., Cavender-Bares, J., 2011. Southward pleistocene migration of Douglas-fir into Mexico: phylogeography, ecological niche modeling, and conservation of 'rear edge' populations. New Phytol. 189, 1185–1199.

Guiher, T.J., Burbrink, F.T., 2008. Demographic and phylogeographic histories of two venomous North American snakes of the genus *Agkistrodon*. Mol. Phylogenet. Evol. 48, 543–553.

Guillette, L.J., Smith, H.M., 1982. A review of the Mexican lizard *Barisia imbricata*, and the description of a new subspecies. Trans. Kansas Acad. Sciences 85, 13–33.

Hewitt, G.M., 1996. Some genetic consequences of ice ages, and their role in divergence and speciation. Biol. J. Linn. Soc. 58, 247–276.

Hewitt, G.M., 2000. The genetic legacy of the Quaternary ice ages. Nature 405, 907–913.

Hewitt, G.M., 2004, Genetic consequences of climatic oscillations in the Quaternary. Philos. Trans. R. Soc. London B, 359, 183-195.

Hillis, D.M., Bull, J.J., 1993. An empirical test of bootstrapping as a method for assessing confidence in phylogenetic analysis. Syst. Biol. 42, 182–192.

Ho, S.Y.W., 2005. Time dependency of molecular rate estimates and systematic overestimation of recent divergence times. Mol. Biol. Evol. 22, 1561–1568.

Ho, S.Y.W., Phillips, M.J., 2009. Accounting for calibration uncertainty in phylogenetic estimation of evolutionary divergence times. Syst. Biol. 58, 367–380.

Holman, J.A., 1970. A Pleistocene herpetofauna from Eddy County, New Mexico. Texas J. Sci. 22, 29–39.

Holman, J.A., 1995. Pleistocene Amphibians and Reptiles of North America. Oxford, NY: Oxford University Press.

Horowitz, S.B., 1955. An arrangement of the subspecies of the horned toad, *Phrynosoma orbiculare* (Iguanidae). Am. Mid. Nat. 54, 204–218.

Hudson, R.R., Coyne, J.A., 2002. Mathematical consequences of the genealogical species concept. Evolution 56, 1557–1565.

Hulsey, C.D., García de León, F.J., Johnson, Y.S., Hendrickson, D.A., Near, T.J., 2004. Temporal diversification of Mesoamerican cichlid fishes across a major biogeographic boundary. Mol. Phylgenet. Evol. 31, 754–764.

Jones, K.B., 1995. Phylogeography of the desert horned lizard (*Phrynosoma platyrhinos*) and the short-horned lizard (*Phrynosoma douglassi*): Patterns of divergence and diversity. PhD Thesis, University of Nevada, Las Vegas.

Kelly, C.M.R., Barker, N.P., Villet, M.H., Broadley, D.G., 2009. Phylogeny, biogeography and classification of the snake superfamily Elapoidea: a rapid radiation in the late Eocene. Cladistics 25, 38–63.

Kerhoulas, N.J., Arbogast, B.S., 2010. Molecular systematics and Pleistocene biogeography of Mesoamerican flying squirrels. J. Mammal. 91, 654-667.

Kuriyama, T., Brandley, M.C., Katayama, A., Mori, A., Honda, M., Hasegawa, M., 2011. A time-calibrated phylogenetic approach to assessing the phylogeography and colonization history of snakes in the Japanese Izu Islands. J. Biogeogr. 38, 259–271.

Lamb, T., Avise, J.C., Gibbons, J.W., 1989. Phylogeographic patterns in mitochondrial DNA of the desert tortoise (*Xerobates agassizi*), and evolutionary relationships among the North American desert tortoises, Evolution 43, 76–87.

Leaché, A.D., McGuire, J.A., 2006. Phylogenetic relationships of horned lizards (*Phrynosoma*) based on nuclear and mitochondrial data: evidence for a misleading mitochondrial gene tree. Mol. Phylogenet. Evol. 39, 628–644.

Leaché, A.D., Mulcahy, D.G., 2007. Phylogeny, divergence times, and species limits of spiny lizards (*Sceloporus magister* species group) in western North American deserts and Baja California. Mol. Ecol. 16, 5216–5233.

Lemos-Espinal, J.A., Smith, H.M., 2007a. Anfibios y Reptiles del Estado de Chihuahua, México/Amphibians and Reptiles of the State of Chihuahua, México. CONABIO, México, D.F.

Lemos-Espinal, J.A., Smith, H.M., 2007b. Anfibios y Reptiles del Estado de Coahuila, México/Amphibians and Reptiles of the State of Coahuila, México. CONABIO, México, D.F.

León-Paniagua, L., Navarro-Sigüenza, A.G., Hernández-Baños, B.E., Morales, J.C., 2007. Diversification of the arboreal mice of the genus *Habromys* (Rodentia: Cricetidae: Neotominae) in the Mesoamerican highlands. Mol. Phylgenet. Evol. 42, 653–664.

Lindell, J., Méndez-de la Cruz, F.R., Murphy, R.W., 2008. Deep biogeographical history and cytonuclear discordance in the black-tailed brush lizard (*Urosaurus nigricaudus*) of Baja California. Biol. J. Linnaean Soc. 94, 89–104.

Luna-Vega, I., Alcántara-Ayala, O., Espinosa-Organista, D., Morrone, J.J., 1999. Historical relationships of the Mexican cloud forests: a preliminary vicariance model applying Parsimony Analysis of Endemicity to vascular plant taxa, J. Biogeogr. 26, 1299–1305.

Luxbacher, A.M., Knouft, J.H., 2009. Assessing concurrent patterns of environmental niche and morphological evolution among species of horned lizards (*Phrynosoma*). J. Evol. Biol. 22, 1669–1678.

Macey, J.R., Wang, Y., Ananjeva, N.B., Larson, A., Papenfuss, T.J., 1999. Vicariant patterns of fragmentation among gekkonid lizards of the genus *Teratoscincus* produced by the Indian Collision: a molecular phylogenetic perspective and an area cladogram for Central Asia. Mol. Phylogenet. Evol. 12, 320–332.

Marshall, C.J., Liebherr, J.K., 2000. Cladistic biogeography of the Mexican Transition Zone. J. Biogeogr. 27, 203–216.

Mateos, M., 2005. Comparative phylogeography of the genera *Poecilia* and *Poeciliopsis* in Central Mexico. J. Biogeography 32, 775–780.

Mateos, M., Sanjur, O.I., Vrijenhoek, R.C., 2002. Historical biogeography of the fish genus *Poeciliopsis* (Cyprinodontiformes). Evolution 56, 972–984.

McCormack, J.E., Peterson, A.T., Bonaccorso, E., Smith, T.B., 2008. Speciation in the highlands of Mexico: genetic and phenotypic divergence in the Mexican jay (*Aphelocoma ultramarina*). Mol. Ecol. 17, 2505–2521.

McCormack, J.E., Zellmer, A.J., Knowles, L.L., 2010. Does niche divergence accompany allopatric divergence in *Aphelocoma* jays as predicted under ecological speciation?: Insights from tests with niche models. Evolution 64, 1231–1244.

McCormack, J.E., Heled, J., Delaney, K.S., Peterson, A.T., Knowles, L.L., 2011. Calibrating divergence times on species trees versus gene trees: implications for speciation history of *Aphelocoma* jays. Evolution 65, 184–202.

McDiarmid, R.W., 1963. A collection of reptiles and amphibians from the highland faunal assemblage of western Mexico. Contrib. Sci. Los Angeles Co. Mus. 68, 1–15.

McDonald, J.A., 1993. Phytogeography and history of the alpine–subalpine flora of northeastern Mexico. In: Biological Diversity of Mexico: Origins and Distribution, pp. 681–703. Edited by: Ramamoorthy, T.P., Bye, R.A., Lot, A., Fa, J. Oxford, NY: Oxford University Press.

Mendoza-Quijano, F., Mejenes, A.S.M.L., Reynoso-Rosales, V.H., Estrada, M.A.H., Rodríguez, M.B., 2001. Anfibios y reptiles de la sierra de Santa Rosa, Guanajuato: cien años después. Anales del Instituto de Biología Universidad Nacional Autónoma de México, Serie Zoología 72, 233–243.

Mendoza-Quijano, F., Vázquez Díaz, J., Quintero Díaz, G.E., 2007. *Phrynosoma orbiculare*. In: IUCN 2010. IUCN Red List of Threatened Species. Version 2010.4.

Metcalfe, S.E., O'Hara, S.L., Caballero, M., Davies, S.J., 2000. Records of Late Pleistocene-Holocene climatic change in Mexico—a review. Quaternary Sci. Rev. 19, 699–721.

Mittermeier, R.A., Gil, P.R., Hoffman, M., Pilgrim, J., Brooks, T., Mittermeier, C.G., Lamoreux, J., da Fonseca, G.A.B., 2005. Hotspots Revisited: Earth's Biologically Richest and Most Endangered Terrestrial Ecoregions. Conservation International, Washington, D.C.

Montanucci, R.R., 1979. Notes on systematics of homed lizards allied to *Phrynosoma orbiculare* (Lacertilia: Iguanidae). Herpetologica 35, 116–124.

Montanucci, R.R., 1987. A phylogenetic study of the horned lizards, genus *Phrynosoma*, based on skeletal and external morphology. Contrib. Sci. Nat. Hist. Mus. Los Angeles Co. 390, 1–36.

Moore, B.R., Chan, K.M.A., 2007. SymmeTREE: An application for performing whole-tree tests of diversification, version 1.1. User manual. http://www.phylodiversity.net/brian/software_symmetree.html.

Moore, W.S., 1995. Inferring phylogenies from mtDNA variation: mitochondrial gene trees versus nuclear gene trees. Evolution 49, 718–726.

Morafka, D.J., 1977. A biogeographical analysis of the Chihuahuan Desert through its herpetofauna. Biogeographica 9, 1–313.

Morando, M., Avila, L.J., Baker, J., Sites, Jr. J.W., 2004. Phylogeny and phylogeography of the *Liolaemus darwinii* complex (Squamata: Liolaemidae): evidence for introgression and incomplete lineage sorting. Evolution 58, 842–876.

Moreno-Letelier, A., Piñero, D., 2009. Phylogeographic structure of *Pinus strombiformis* Engelm. across the Chihuahuan Desert filter-barrier. J. Biogeogr. 36, 121–131.

Mulcahy, D.G., Mendelson, J.R. III, 2000. Phylogeography and speciation of the morphologically variable, widespread species *Bufo valliceps*, based on molecular evidence from mtDNA. Mol. Phylgenet. Evol. 17, 173–189.

Mulcahy, D.G., Morrill, B.H., Mendelson, J.R. III, 2006. Historical biogeography of lowland species of toads (*Bufo*) across the Trans-Mexican Neovolcanic Belt and the Isthmus of Tehuantepec. J. Biogeogr. 33, 1889–1904.

Mulcahy, D.G., Spaulding, A., Mendelson, J.R., Brodie Jr., E.D., 2006. Phylogeography of the Flat-tailed Horned lizard (*Phrynosoma mcallii*) and systematics of the *P. mcallii–platyrhinos* mtDNA complex. Mol. Ecol. 15, 1807–1826.

Murphy, R.W., Trepanier, T.L., Morafka, D.J., 2006. Conservation genetics, evolution and distinct population segments of the Mojave fringe-toed lizard, *Uma scoparia*. J. Arid Environ. 67, 226–247.

Neiswenter, S.A., Riddle, B.R., 2010. Diversification of the *Perognathus flavus* species group in emerging arid grasslands of western North America. J. Mammal. 91, 348–362.

Nylander, J.A.A., 2004. MRMODELTEST v2. Program distributed by the author. Evolutionary Biology Centre, Uppsala University, Uppsala.

Nylander, J.A.A., Wilgenbusch, J.C., Warren, D.L., Swofford, D.L., 2008. AWTY (are we there yet?): a system for graphical exploration of MCMC convergence in Bayesian phylogenetic inference. Bioinformatics 24, 581–583.

Paniagua, L.L., Morrone, J.J., 2009. Do the Oaxacan Highlands represent a natural biotic unit? A cladistic biogeographical test based on vertebrate taxa. J. Biogeogr. 36, 1939–1944.

Pellmyr, O., Segraves, K.A., 2003. Pollinator divergence within an obligate mutualism: two yucca moth species (Lepidoptera; Prodoxidae: *Tegeticula*) on the Joshua tree (*Yucca brevifolia*; Agavaceae). Annals Entomol. Soc. America 96, 716–722.

Peterson, A.T., Flores-Villela, O.A., León-Paniagua, L.S., Llorente- Bousquets, J.E., Luis-Martinez, M.A., Navarro-Siguenza, A.G., Torres-Chavez, M.G., Vargas-Fernandez, I., 1993. Conservation priorities in northern Middle America: moving up in the world. Biodiversity Letters 1, 33–38.

Presch, W., 1969. Evolutionary osteology and relationships of the horned lizard genus *Phrynosoma* (Family Iguanidae). Copeia 1969, 250–275.

Pyron, R.A., Burbrink, F.T., 2009. Lineage diversification in a widespread species: roles for niche divergence and conservatism in the common kingsnake, *Lampropeltis getula*. Mol. Ecol. 18, 3443–3457.

Pyron, R.A., Burbrink, F.T., 2010. Hard and soft allopatry: physically and ecologically mediated modes of geographic speciation. J. Biogeogr. 37, 2005–2015.

Rabosky, D.L., 2006a. Likelihood methods for inferring temporal shifts in diversification rates. Evolution 60, 1152–1164.

Rabosky, D.L., 2006b. LASER: a maximum likelihood toolkit for detecting temporal shifts in diversification rates from molecular phylogenies. Evol. Bioinformatics Online 2, 257–260.

Ramamoorthy, T., Bye, R., Lot, A., Fa, J., 1993. Biological Diversity of Mexico: Origins and Distribution. Oxford University Press, Oxford.

Rambaut, A., Drummond, A.J., 2007. TRACER v1.4. Available at: http://beast.bio.ed.ac.uk/Tracer

Ree, R.H., Smith, S.A., 2008. Maximum-likelihood inference of geographic range evolution by dispersal, local extinction, and cladogenesis. Sys. Biol. 57, 4–14.

Riddle, B.R., Hafner, D.J., Alexander, L.F., Jaeger, J.R., 2000a. Cryptic vicariance in the historical assembly of a Baja California peninsular desert biota. Proc Natl Acad Sci USA 97, 14438–14443.

Riddle, B.R., Hafner, D.J., Alexander, L.F., 2000b. Phylogeography and systematics of the *Peromyscus eremicus* species group and the historical biogeography of North American warm regional deserts. Mol. Phylogenet. Evol. 17, 145–160.

Riddle, B.R., Dawson, M.N., Hadly, E.A., Hafner, D.J., Hickerson, M.J., Mantooth, S.J., Yoder, A.D., 2008. The role of molecular genetics in sculpting the future of integrative biogeography. Progress Phys. Geogr. 32, 173–202.

Robinson, M.D., Van Devender, T.R., 1973. Miocene lizards from Wyoming and Nebraska. Copeia 1973, 698–704.

Rogers, K.L., 1976. Herpetofauna of the Beck Ranch local fauna (upper Pliocene: Blancan) of Texas. Publ. Mus. Michigan State Univ. Paleontological Ser. 1, 167–200.

Ronquist, F., Huelsenbeck, J.P., 2003. MRBAYES 3: Bayesian phylogenetic inference under mixed models. Bioinformatics 19, 1572–1574.

Rosas-Elguera, J., Alva-Valdivia, L., Goguitchaichvili, A., et al., 2003. Counterclockwise rotation of the Michoacan Block: implications for the tectonics of western Mexico. Int. Geol. Rev. 45, 814–826.

Ruiz, E.A., Rinehart, J.E., Hayes, J.L., Zuñiga, G., 2010. Historical demography and phylogeography of a specialist bark beetle, *Dendroctonus pseudotsugae* Hopkins (Curculionidae: Scolytinae). Environ. Entomol. 39, 1685–1697.

Salinas-Moreno, Y., Mendoza-Correa, G., Barrios, M.A., Cisneros, R., Macías-Sámano, J., Zúñiga, G., 2004. Areography of the genus *Dendroctonus* (Coleoptera: Curculionidae: Scolytinae) in México. J. Biogeogr. 31, 1163–1177.

SEMARNAT, 2010. Norma Oficial Mexicana NOM-059-SEMARNAT-2010, Protección ambiental-Especies nativas de México de flora y fauna silvestres-Categorías de riesgo y especificaciones para su inclusión, exclusión o cambio-Lista de especies en riesgo. México. Jueves 30 de diciembre de 2010.

Shafer, A.B.A., Cullingham, C.I., Côté, S.D., Coltman, D.W., 2010. Of glaciers and refugia: A decade of study sheds new light on the phylogeography of northwestern North America. Mol. Ecol. 19, 4589–4621.

Sherbrooke, W.C., 2003. Introduction to Horned Lizards of North America. University of California Press, CA.

Sinervo, B., Méndez de la Cruz, F., Miles, D.B., et al., 2010. Erosion of lizard diversity by climate change and altered thermal niches. Science 328, 894–899.

Smith, H.M., Camarillo, J.L.R., Chiszar, D., 1993. The status of the members of the *Sceloporus aeneus* complex (Reptilia: Sauria) of Mexico. Bull. Maryland Herpetol. Soc. 29, 130–139.

Smith, H.M., Watkins-Colwell, G.J., Liner, E.A., Chiszar, D., 1996. *Sceloporus scalaris* auctorum a superspecies (Reptilia: Sauria). Bull. Maryland. Herpetol. Soc. 32, 70–74.

Smith, H.M., Watkins-Colwell, G.J., Lemos-Espinal, J.A., Chiszar, D., 1997. A new subspecies of the lizard *Sceloporus scalaris* (Reptilia: Sauria: Phrynosomatidae) from the Sierra Madre Occidental of Mexico. Southwest. Nat. 42, 290–301.

Soltis, D.E., Morris, A., McLachlan, J.S., Manos, P.S., Soltis, P.S., 2006. Comparative phylogeography of unglaciated eastern North America. Mol. Ecol. 15, 4261–4293.

Stamatakis, A., 2006. RAxML-VI-HPC: Maximum likelihood-based phylogenetic analyses with thousands of taxa and mixed models. Bioinformatics 22, 2688–2690.

Sullivan, J., Arellano, E., Rogers, D.S., 2000. Comparative phylogeography of Mesoamerican highland rodents: concerted versus independent response to past climatic fluctuations. Am. Nat. 155, 755–768.

Tennessen, J.A., Zamudio, K.R., 2008. Genetic differentiation among mountain island populations of the striped plateau lizard, *Sceloporus virgatus* (Squamata: Phrynosomatidae). Copeia 2008, 558–564.

Upton, D.E., Murphy, R.W., 1997. Phylogeny of the side-blotched lizards (Phrynosomatidae: *Uta*) based on mtDNA sequences: support for a midpeninsular seaway in Baja California. Mol. Phylgenet. Evol. 8, 104–113.

Van Devender, T.R., Eshelman, R.E., 1979. Referral of the fossil lizard *Sceloporus holmani* (late Pliocene of north-central Kansas) to the genus *Phrynosoma*. Herpetologica 35, 380–382.

Watkins-Colwell, G.J., Smith, H.M., Chiszar, D., 1996. Geographic distribution. *Sceloporus scalaris scalaris*. Herpetol. Rev. 27, 153.

Watkins-Colwell, G.J., Smith, H.M., Chiszar, D., 2005. *Sceloporus scalaris*. Cat. Am. Amphibians Reptiles 814, 1–10.

Webb, T. III, Bartlein, P.J., 1992. Global changes during the last 3 million years, climatic controls and biotic responses. Annu. Rev. Ecol. Syst. 23, 141–173.

Weir, J.T., Bermingham, E., Miller, M.J., Klicka, J., González, M.A., 2008. Phylogeography of a morphologically diverse Neotropical montane species, the common bush-tanager (*Chlorospingus ophthalmicus*). Mol. Phylogenet. Evol. 47, 650–664.

Wiens, J.J., 2004. Speciation and ecology revisited: phylogenetic niche conservatism and the origin of species. Evolution 58, 193–197.

Wiens, J.J., Reeder, T.W., 1997. Phylogeny of the spiny lizards (*Sceloporus*) based on molecular and morphological evidence. Herpetol. Monog. 11, 1–101.

Wiens, J.J., Parra-Olea, G., García-París, M., Wake, D.B., 2007. Phylogenetic history underlies elevational patterns of biodiversity in tropical salamanders. Proc. R. Soc. London 274, 919–928.

Wiens, J.J., Kuczynski, C.A., Arif, S., Reeder, T.W., 2010. Phylogenetic relationships of phrynosomatid lizards based on nuclear and mitochondrial data, and a revised phylogeny for *Sceloporus*. Mol. Phylgenet. Evol. 54, 150–161.

Yatkola, D.A., 1976. Mid-Miocene lizards from Western Nebraska. Copeia 1976, 645–654.

Zaldivar-Riverón, A., Nieto-Montes de Oca, A., 2002. Variation in the rare lizard *Barisia rudicollis* (Anguidae) (Wiegmann) with the description of a new species from Central Mexico. Herpetologica 58, 313–326.

Zaldivar-Riverón, A., Nieto-Montes de Oca, A., Laclette, J.P., 2005. Phylogeny and evolution of dorsal pattern in the Mexican endemic lizard genus *Barisia* (Anguidae: Gerrhonotinae). J. Zoo. Syst. Evol. Res. 43, 243–257.

Zink, R.M., Barrowclough, G.F., 2008. Mitochondrial DNA under siege in avian phylogeography. Mol. Ecol. 17, 2107–2121.

VITA

Graduate College
University of Nevada Las Vegas

Robert W. Bryson, Jr.

Degrees:

Bachelor of Science, 1998
Sul Ross State University, Alpine, TX

Master of Science, 2002
Sul Ross State University, Alpine, TX

Select First-authored Publications:

Bryson R. W., R. W. Murphy, M. R. Graham, A. Lathrop, and D. Lazcano-Villareal. In press. Historical diversification of the *Crotalus intermedius* group and Pleistocene pine-oak woodland connections between Mexico's Sierra Madre Occidental and Sierra Madre Oriental. Journal of Biogeography.

Bryson, R. W., U. O. García-Vázquez, and B. R. Riddle. 2011. Phylogeography of Middle American gophersnakes: mixed responses to biogeographical barriers across the Mexican Transition Zone. Journal of Biogeography 38: 1570-1584.

Bryson, R. W., R. W. Murphy, A. Lathrop, and D. Lazcano-Villareal. 2011. Evolutionary drivers of phylogeographical diversity in the highlands of Mexico: a case study of the *Crotalus triseriatus* species group of montane rattlesnakes. Journal of Biogeography 38: 697-710.

Bryson, R. W., A. Nieto-Montes de Oca, J. R. Jaeger, and B. R. Riddle. 2010. Elucidation of cryptic diversity in a widespread Nearctic treefrog reveals episodes of mitochondrial gene capture as frogs diversified across a dynamic landscape. Evolution 64: 2315-2330.

Bryson, R. W., and M. R. Graham. 2010. A new alligator lizard from northeastern Mexico. Herpetologica 66: 92-98.

Bryson, R. W., J. M. Mueller, and D. Lazcano. 2008. Observations on the thermal ecology of montane Mexican rattlesnakes, p. 287–290. In: The Biology of the Rattlesnakes. W. K. Hayes, K. R. Beaman, M. D. Cardwell, and S. P. Bush (eds.).

Bryson, R. W., A. Nieto-Montes, and J. Reyes-Velasco. 2008. Phylogenetic position of *Porthidium hespere* (Viperidae: Crotalinae) and phylogeography of arid-adapted hognosed pitvipers based on mitochondrial DNA. Copeia 2008: 170-176.

Bryson, R. W., and F. Mendoza-Quijano. 2007. Cantils of Hidalgo and Veracruz, Mexico, with comments on the validity of *Agkistrodon bilineatus lemosespinali*. Journal of Herpetology 41: 536-539.

Bryson, R. W., J. Pastorini, F. T. Burbrink, and M. R. J. Forstner. 2007. A phylogeny of the *Lampropeltis mexicana* complex (Serpentes: Colubridae) based on mitochondrial DNA sequences suggests evidence for species-level polyphyly within Lampropeltis. Molecular Phylogenetics and Evolution 43: 674-684.

Bryson, R. W., H. M. Smith, and J. Lemos-Espinal. 2005. Taxonomic status of the Madrean alligator lizard of the Sierra del Nido, Chihuahua, México (Lacertilia: Anguidae). Southwestern Naturalist 50: 497-498.

Bryson, R. W., J. R. Dixon, and D. Lazcano. 2005. New species of *Lampropeltis* (Serpentes: Colubridae) from the Sierra Madre Occidental, México. Journal of Herpetology 39: 207-214.

Bryson, R. W., G. Ulises, and D. Lazcano. 2003. Observations on a population of Mexican lance-headed rattlesnake (*Crotalus polystictus*) from an agricultural area in the Mexican state of México. Herpetological Review 34: 313-314.

Bryson, R. W., and D. Lazcano. 2002. Reproduction and mating behavior in the Del Nido ridgenose rattlesnake, *Crotalus willardi amabilis*. Southwestern Naturalist 47: 310-311.

Dissertation Title: Historical Diversification of Montane Herpetofauna Within and Between the Sierras of Mexico

Dissertation Examination Committee:

Chair, Dr. Brett R. Riddle
Committee Member, Dr. John Klicka
Committee Member, Dr. Brian Hedlund
Outside Committee Member, Dr. Jonathan A. Campbell
Graduate Faculty Representative, Dr. Steve Rowland